DOUBLY FED INDUCTION MOTOR USING SCR INVERTER

A Thesis

Submitted to the Faculty of Graduate Studies

in Partial Fulfilment of the Requirements

for the Degree of

Master of Science

in the Department of Electrical Engineering

University of Saskatchewan

by

NARAYAN S. RAU

Saskatoon, Saskatchewan

December, 1965

ACKNOWLEDGEMENTS

The author is grateful to Prof. R.J. Fleming for his guidance during the course of this work. The helpful discussions with Prof. A.G. Wacker in certain phases of the work on inverters is gratefully acknowledged.

This work was supported by the National Research Council of Canada under Grant No. A-1542.

UNIVERSITY OF SASKATCHEWAN

Electrical Engineering Abstract 65A81

"DOUBLY FED INDUCTION MOTOR

USING SCR INVERTER"

Student: Narayan S. Rau Supervisor: R.J. Fleming

M.Sc. Thesis presented to College of Graduate Studies
December 1965.

ABSTRACT

Direct current drive schemes have been employed in the past for industrial applications where closely controlled torque-speed characteristics were necessary. Alternating current drive schemes, which offer the advantages of simplicity of operation and maintenance have not been able to give similar torque-speed characteristics without the use of auxiliary commutator machines. Attempts to employ the induction motor as a variable speed drive using static devices as control elements have met with some success.

This thesis presents an analysis of the characteristics of a three phase induction motor drive where the stator and the rotor are both fed with energy, the stator from the supply mains and the rotor through a bridge connected silicon controlled inverter. The necessary analysis of the inverter operation, the torque calculations with the inverter in the rotor circuit and the design of a suitable control circuit for the control of the drive scheme are presented. This thesis also outlines the tests which were performed in the laboratory to check the accuracy of the analysis of the inversion process and the motor torque calculations.

The results of this preliminary study are encouraging and indicate that this scheme offers possibilities for dynamic braking of hoisting and traction type loads. A number of aspects which require further investigation are outlined.

This research was supported by the National Research Council under Grant A-1542

TABLE OF CONTENTS

		Page
Acknowledgements		ii
Abstract		iii
Table of Contents		iv
List of Figures		vi
List of Tables		viii
List of Symbols		ix
1.	INTRODUCTION	
1.1	Background	1.
1.2	The Problem	3.
2.	EQUIVALENT CIRCUIT OF THREE PHASE BRIDGE INVERTER	
2.1	Introduction	6.
2.2	Operation of Rectifiers and Inverters	6.
2.2.1	Conditions for conduction	6.
2.2.2	Rectification	9.
2.2.3	Inversion	11.
2.3	Analysis of Conduction	13.
2.4	Conduction Equations	16.
2.4.1	Interval 1	16.
2.4.2	Interval 2	17.
2.4.3	Interval 3	19.
2.4.4	Interval 4	20.
2.4.5	Interval 5	22.
2.5	Solution of Conduction Equations	23.
2.6	The Equivalent Circuit	25.
2.7	Analysis of Conduction Equations	26.
3.	INVERTER IN THE ROTOR OF A THREE PHASE INDUCTION MOTOR	
3.1	Generalized Equations of an Induction Motor	30.
3.1.1	The circuit for analysis	30.
3.1.2	Induction motor as a generalized machine	35.
3.2	Generalized Equations Applied to Motor with the Inverter in the Rotor	38.
3.3	Torque Calculations	41.
3.4	Torque Tensor	46.

TABLE OF CONTENTS (CONT'D)

		Page
4.	EXPERIMENTAL INVESTIGATIONS	
	4.1 Physical Test Setup	48.
	4.2 Summary of Test Procedure	
	4.2.1 Outline	51.
	4.2.2 Tests to study the behaviour of the inverter	52.
	4.2.3 Torque measurements of the motor under standstill conditions	59.
	4.2.4 Speed torque characteristics	61.
5.	CONCLUSIONS AND RECOMMENDATIONS	
	5.1 Conclusions	
	5.1.1 Conduction equations	65.
	5.1.2 Torque equations	65.
	5.1.3 Drive characteristics	65.
	5.2 Recommendations for Further Work	66.
	5.3 Concluding Remarks	66.
6.	REFERENCES	68.
7.	APPENDICES	
	7.1 Note on the Design of the Firing Control Circuit	70.
	7.1.1 Requirements of firing circuit	70.
	7.1.2 Operation of the firing circuit	70.
	7.2 Solution of the Conduction Differential Equations	77.
	7.3 Digital Computer Program for the Solution of Conduction Equations	82.
	7.4 Transformation of Phase Currents to d and q Axes of an Induction Motor	89.
	7.4.1 d and q transformations of the induction motor	89.
	7.4.2 Evaluation of the constant K	91.
	7.5 Solution of Torque Equations	92.
	7.6 Digital Computer Program for the Solution of Stator d and q Currents	96.
	7.7 Transformation of Rotor Harmonic Currents to Two Synchronously Rotating Axes	96.

LIST OF FIGURES

Fig.		Page
1.1	General scheme of the drive	4.
2.1	Bridge rectifier	7.
2.2	Bridge inverter	7.
2.3	Process of rectification and inversion in relation to voltage	8.
2.4	Circuit conditions prior to interval 1	15.
2.5	Circuit conditions during interval 1	15.
2.6	Circuit conditions during interval 2	18.
2.7	Circuit conditions during interval 3	18.
2.8	Circuit conditions during interval 4	21.
2.9	Circuit conditions during interval 5	21.
2.10	Circuit at the instant of switching element 2	27.
2.11	Equivalent circuit of a bridge inverter	28.
2.12	Current components during intervals	28.
3.1	Equivalent circuit of motor	32.
3.2	Equivalent circuit with inverter in the rotor	32.
3.3	Equivalent circuit of motor - alternative form	33.
3.4	Generalized machine - fixed reference axes	36.
3.5	Generalized machine - rotating reference axes	36.
3.6	Vectorial representation of harmonic currents	44.
4.1	Physical test setup	49.
4.2	Equivalent circuit of experimental motor	53.
4.3	Inverter current conduction pattern at standstill	55.

LIST OF FIGURES (CONT'D)

Fig.		Page
4.4	Current pattern during inversion at s = 0.5	57.
4.5	Torque speed relations	62.
7.1	Wave shapes and pulse relations	71.
7.2	The firing circuit	73.
7.3	Control circuit waveforms	75.
7.4	Block diagrams of logic for the solution of conduction equations	83.
7.5	Block diagram of logic for the solution of torque equations	97.

LIST OF TABLES

Table		Page
2.1	Summary of Conduction Equations	24.
4.1	Comparison of Torque Values	60.
7.1	Card Listings of the Program for the Solution of Conduction Equations	84.
7.2	Card Listings of the Program for the Solution of Torque Equations	98.
7.3	Output From the Computer	101.

LIST OF SYMBOLS

Symbols:

C_1 to C_5	Constant of integration
I	Current (Amperes)
i	Current in equivalent machine (Amperes)
L	Inductance (Henries)
M	Mutual inductance (Henries)
R	Resistance (Ohms)
s	Slip of induction motor
V	Voltage (Volts)
X	Reactance (Ohms)
Z	Impedance (Ohms)
β	Delay in firing elements or the firing angle (Radians) (Fig. 2.3)
γ	Commutation angle (Radians)
ϕ	Phase Angle (Radians)
ω	Angular velocity (Radians/second)

Subscripts:

d	Direct current
ds	Direct axis stator
dr	Direct axis rotor
e	End of interval
m	Maximum value referred to alternating quantity
n	Order of harmonic

LIST OF SYMBOLS (CONT'D)

qs	Quadrature axis stator
qr	Quadrature axis rotor
s	Slip of induction motor
R, Y and B	Phases of phase sequence R, Y and B
1 to 6	Rectifier elements of the bridge
1 to 9	Order of harmonics
(1)..(5)	Conduction intervals

1. INTRODUCTION

1.1 Background

A continuing effort has been made by the electrical industry to replace direct current motors with alternating current motors in rotary drive systems. The a.c. machines are cheaper, more robust and avoid the serious shortcomings of d.c. machines due to mechanical commutation. Above all, the a.c. systems obviate the need for conversion equipment for the supply of d.c. voltages; however, the control characteristics of a.c. motors, especially those of slip ring induction motors which offer the most advantages for these replacements, do not compare favourably with those obtainable with d.c. machines. Accurate speed and/or torque control is required for such drives as reversing drives, hoist and winch drives and traction units. Characteristics that are suitable for these applications can be obtained from an a.c. drive, but the use of auxiliary commutator a.c. machines is necessary. The problems of commutation and the problems of commutator maintenance are associated with these a.c. commutator machines and, therefore, the majority of drives for these applications have been d.c. drives.

The recent developments in the manufacture of solid state rectifiers and the silicon controlled rectifiers have renewed interests in a.c. drive schemes. The developments in this regard can be classified into three major groups:

(1) Drives where the controlled rectifiers control a d.c. machine and work essentially as replacements for the conventional commutators,[1]

(2) Drives where the controlled rectifiers work as a variable frequency a.c. source to provide for variable frequency stator induction motor operation,[2] and

(3) Drives where the controlled rectifiers work mainly as switching elements switching either the stator or the rotor of an induction motor according to a desired scheme.[3,4]

One of the most widely adopted schemes for the speed control of the induction motor is the Cramer drive. The drive consists of an auxiliary commutator machine to rectify the rotor 3 phase voltages of the induction motor. The rectified voltages are fed to a d.c. motor coupled to the shaft of the induction motor. Variations in the field excitations of the d.c. motor result in different speeds of the motor shaft. A modified Cramer drive which could be classified under the last scheme (scheme (3)) consists of a solid state rectifier instead of an auxiliary commutator machine. The d.c. output from the rectifier is either fed to a d.c. motor on the shaft of the induction motor or is fed back to the a.c. supply mains after inversion.

1.2 The Problem

Fig. 1.1 indicates the general scheme of the drive which was studied. The rotor energy, instead of being converted to direct current as in a conventional cramer drive, is derived from a 3 phase bridge inverter. The input to the inverter is from a d.c. source. The induction motor will then be a doubly fed induction motor; the energy being fed to the stator from a three phase a.c. source and to the rotor through a three phase inverter. The frequency and the magnitude of the alternating voltages at the rotor of the induction motor are functions of the angular velocity and the direction of rotation of the rotor. The frequency of the rotor voltages varies from about a cycle per second, corresponding to the operating speed of the motor, to about twice the supply frequency, corresponding to plugging conditions at full forward speed. The control of the inverter must, therefore, make it possible to feed the a.c. energy into the rotor of the motor at the correct frequency and voltage at all speeds.

The equivalent circuit of an induction motor is a useful tool for the computation of steady state torque characteristics; however, before the torque characteristics of a drive as shown in Fig. 1.1 can be investigated, it is necessary to represent the inverter by its equivalent circuit. The purpose of the study, in general terms, was to investigate the behaviour of the inverter in such an application and the torque and speed control possibilities of such a system.

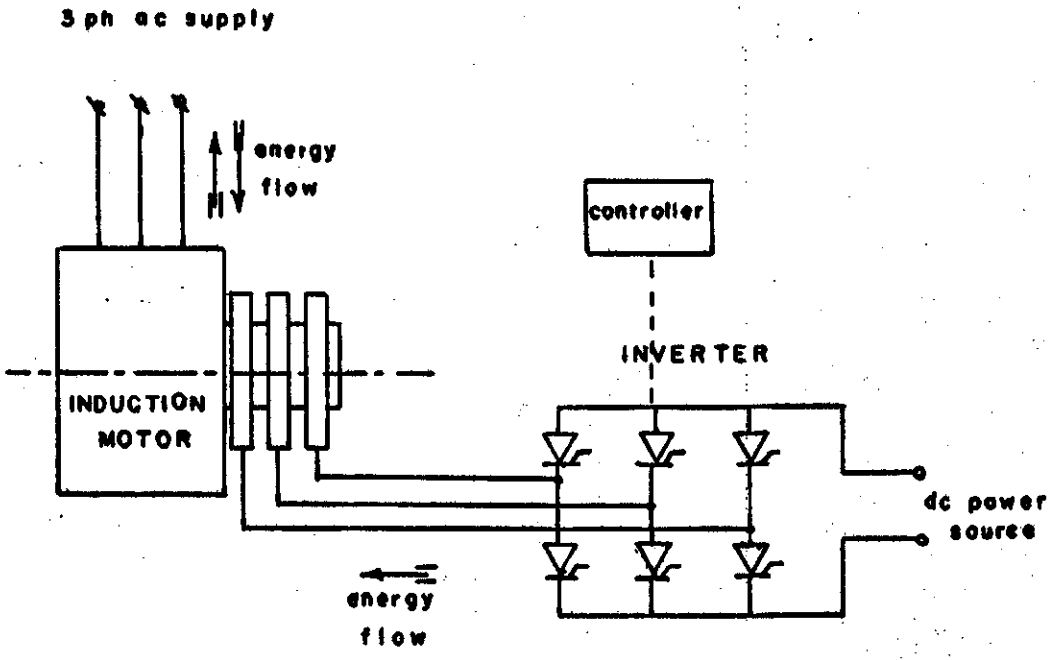

FIGURE 1-1 : GENERAL SCHEME OF THE DRIVE

This thesis describes the development of an equivalent circuit for a three phase bridge connected inverter, the equations necessary for torque computations and the experimental observations of the characteristics of the drive. The design of a firing circuit for the control of a bridge connected inverter and the computer programs used for establishing the conduction pattern and the torque computation of the motor are included in the appendices.

2. EQUIVALENT CIRCUIT OF THREE PHASE BRIDGE INVERTER

2.1 Introduction

The development of an equivalent circuit for a bridge connected inverter can be based on the piecewise linear analysis of the conduction process through the elements of the inverter. The analysis of conduction yields the current pattern in each element. This can be expressed in its Fourier series form. The Fourier coefficients of the current pattern can be represented by harmonic current sources in the equivalent circuit.

2.2 Operation of Rectifiers and Inverters

2.2.1 Conditions for conduction

Figs. 2.1 and 2.2 show the connections of a rectifier and an inverter. The current conduction pattern of a rectifier and an inverter are shown in Fig. 2.3. The rectifiers and inverters use silicon controlled rectifiers (SCRs) as their elements. The SCR will turn on only if the gate power is supplied to it when the voltage across it is in the direction of the forward bias. The current through it can be considered to be the algebraic sum of the forward and the reverse currents provided the sum of the two currents is in the forward direction. Since an SCR can conduct current only in the forward direction, the reverse current has no existence by itself. If the gate or firing power is removed after the conduction starts, the SCR element switches off when the net

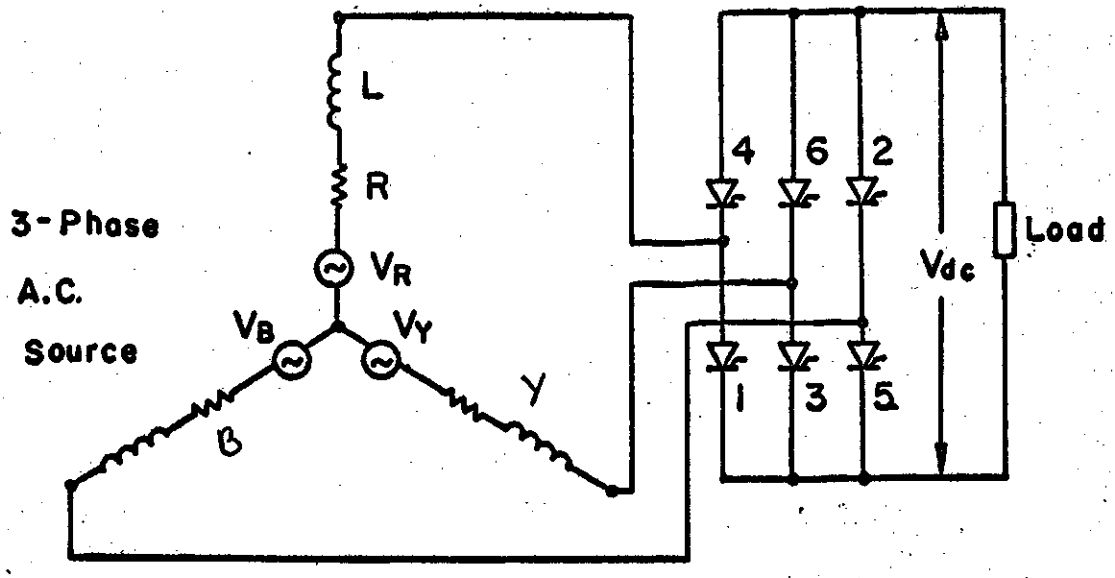

Figure 2-1: Bridge Rectifier

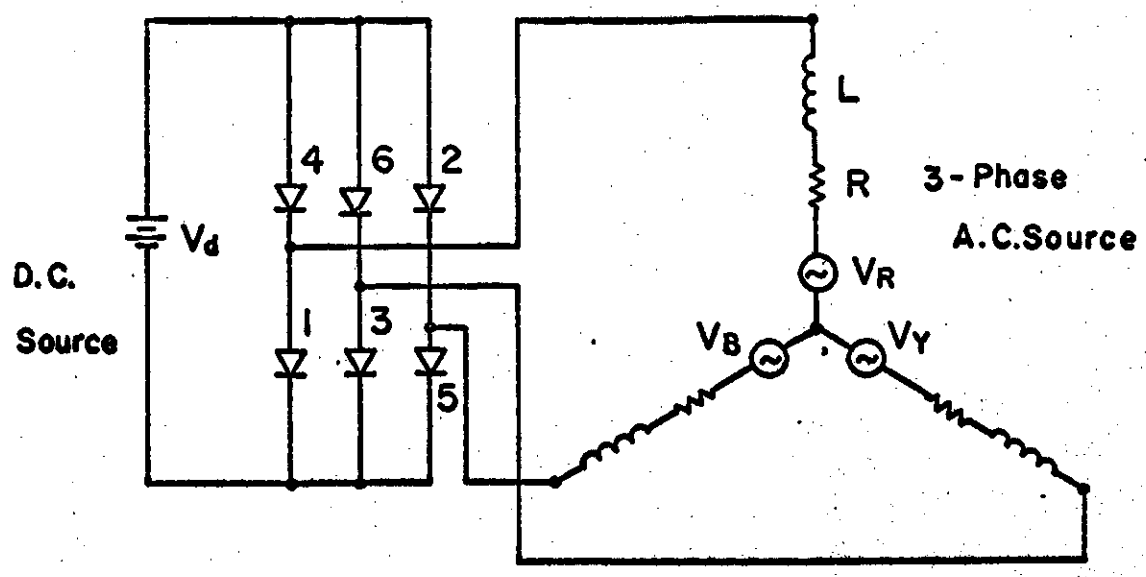

Figure 2-2: Bridge Inverter

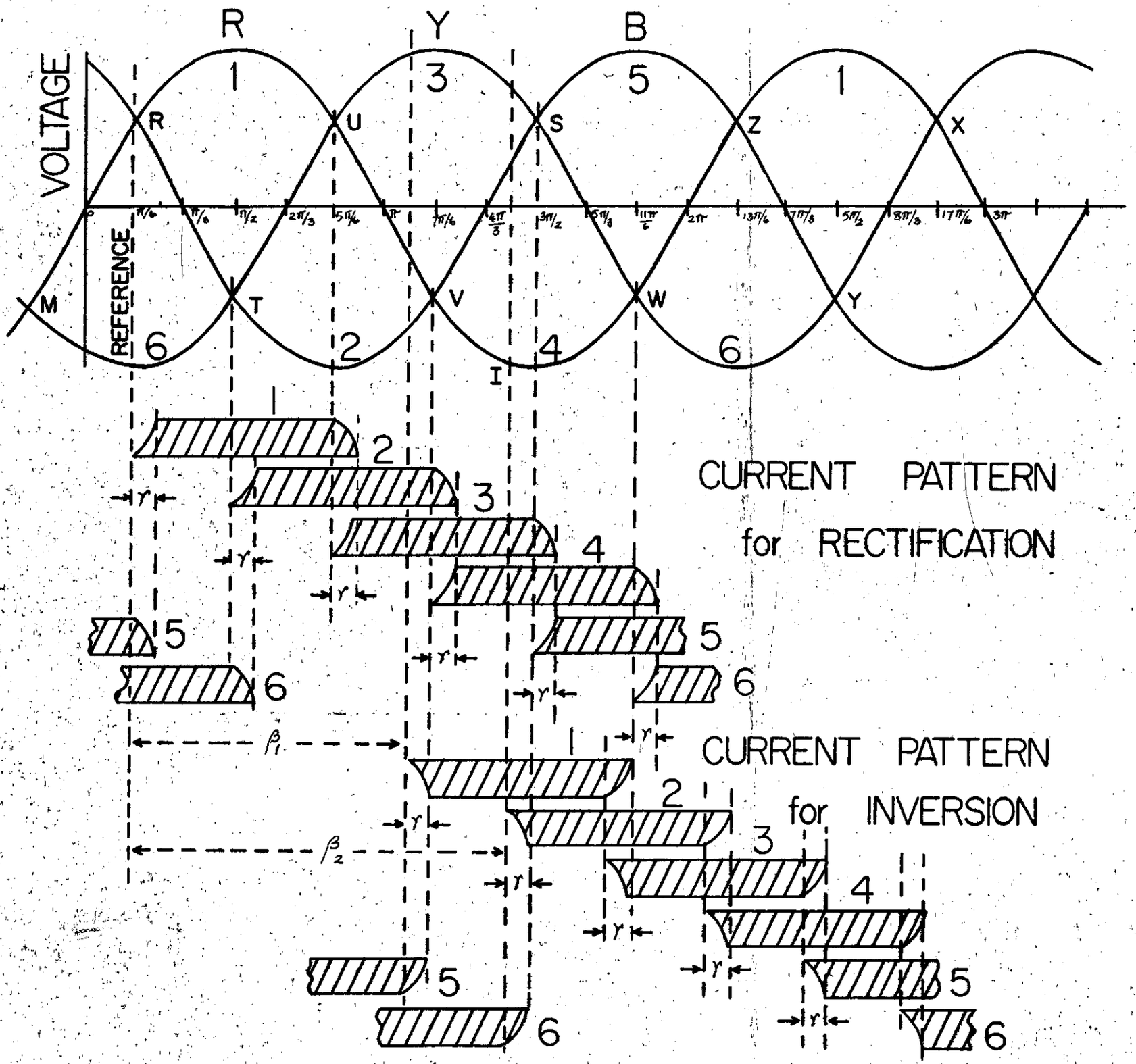

Figure 2.3: Process of Rectification and Inversion In Relation to Voltage.

forward current falls to zero. A rectifier element can, therefore, be considered as a switch which is open or closed depending on whether the net current is in the reverse or the forward direction. In the following analysis, it is assumed that through a suitable firing circuit, the elements are fired sequentially at intervals of 60 electrical degrees with element 1 at zero degrees, element 2 at 60 degrees, etc. The set of firing pulses for the six elements may be translated in time relative to the a.c. voltage wave form. The design and operation of the firing control circuit is discussed in detail in Appendix 7.1.

2.2.2 Rectification

The process of rectification will now be discussed. Referring to Figs. 2.1 and 2.3, if element 6 is fired at the instant M and if element 1 is fired at the instant R as shown in Fig. 2.3, conduction takes place from the R phase of the a.c. source through element 1, external load and element 6 to the Y phase of the a.c. source. The firing pulses for element 6 should be kept positive till element 1 is fired because conduction takes place through both elements 1 and 6 in series and, therefore, the gates of both the elements must be held positive to initiate conduction. For the process of rectification (or inversion as can be seen later) to start, the gate pulses for the SCR elements must be, at least, of 60 degrees duration.

The voltage wave shapes shown in Fig. 2.3 are the voltages of each phase to neutral. The a.c. power source can be represented by an equivalent circuit as shown in Figs. 2.1 and 2.2.

Granted that the conduction is taking place through elements 1 and 6, at the instant T, the voltage of phase B acting through element 2 is becoming more negative than the voltage of phase Y acting through element 6; therefore, if element 2 is fired at instant T, element 2 conducts, taking over conduction from element 6. During this process of the changeover of current conduction, referred to as "commutation", the Y and B phases of the a.c. source are shorted through elements 6 and 2. The short circuit current will be in such a direction as to oppose the current flow in element 6, decreasing the current through element 6 to zero and in the direction of the forward bias of element 2. The commutation of current from element 6 to 2 takes a definite time due to the stored magnetic energy in the inductances of the power source. This delay is designated as γ in Fig. 2.3 and is designated as "angle of overlap" or the "commutation angle". It can be seen in Fig. 2.3 that the current in element 2 is increasing while the current in element 6 is decreasing after instant T. Similarly, at instant U, the voltage of phase Y is becoming more positive than that of phase R. If the element 3 is fired at instant U, commutation takes place from element 1 to 3. Due to the three phase symmetry of the

a.c. source, the commutation angle at instant u is also γ degrees. At instant U, elements 1 and 3 short the R and Y phases of the a.c. power source. Fig. 2.3 shows the decay of current and the increase of current in elements 1 and 3 respectively at instant U. By similar reasoning, it can be shown that elements 4, 5 and 6 will fire at instants V, S and W (Fig. 2.3) resulting in a unidirectional current flow through the external load.

2.2.3 Inversion

The process of inversion will now be described as an extension to the rectification concepts developed in the preceding section. Let conduction be assumed to be taking place between B and Y phases through elements 5 and 6 (Figs. 2.2 and 2.3). If the firing of element 1 is delayed beyond R, the conduction continues between B and Y phases through the elements 5 and 6 until the instant T because, the B phase is positive with respect to Y phase until instant T. If elements 1, 2, 3, 4 and 5 are fired at instants T, V, Y, S and W respectively rather than at R, T, U, V and S as for rectification, the output d.c. voltage falls in spite of the fact that the process of rectification is continuing. Accordingly, if element 1 is fired at instant T, conduction takes place between R and Y phases through elements 1 and 6 as long as the R phase is positive with respect to the Y phase, i.e. until the instant U. The same argument applies to other

elements at successive intervals of time.

If the firing of the element is delayed further, the d.c. output voltage drops more until it attains a value of zero when the elements 1, 2, 3, 4 and 5 are fired at instants U, V, S, W and Z respectively. Under these conditions, the voltage of phase R at the instant of firing element 1, i.e. at instant U, is not positive with respect to the Y phase to which element 6 is connected. Since conduction cannot take place in the reverse direction, i.e. from element 6 to 1, the conduction of current completely stops resulting in zero output d.c. voltage. If the d.c. load has a back emf or if a d.c. source is connected as shown in Fig. 2.2, when element 1 is fired at time U (and, of course, element 6 has been fired 60 degrees prior to U), the d.c. source forces current through elements 1 and 6 into phases R and Y provided the value of the d.c. voltage is high enough to overcome the opposing a.c. voltage acting across R and Y phases. The same reasoning applies at instants V, S, W and Z when the d.c. source forces a current into the a.c. source while the voltage of the a.c. source (line to line voltage) is passing through its negative value. This constitutes inversion and energy derived from the d.c. source is fed into the a.c. source. If the a.c. source is a transformer, the energy is fed back to the a.c. supply mains.

The current pattern for inversion is shown in Fig. 2.3 when elements 1, 2, 3, 4, 5 and 6 are fired at

instants prior to V, S, W, Z, Y and X respectively. The inversion currents are shown as negative in Fig. 2.3.

The process of commutation has to be complete before the instants V, S, W, etc. For example, if the conduction is taking place through elements 5 and 6 during inversion, if element 1 is fired at instant V to take over the conduction from 5, a failure of commutation results because the voltage of R phase after instant V, i.e. the voltage of element 1, is more negative than that of phase B acting through element 5. This means that the current in the loop, B phase--elements 5 and 1--and R phase at instant V (Fig. 2.2) aids the current in element 5 and is in the direction of the reverse bias of 1; therefore, the commutation from element 5 to 1 cannot occur unless the element 1 is fired well before instant V such that the current transfer from element 5 to 1 is complete at the instant V. Fig. 2.3 illustrates inversion when the commutation is just complete at instants V, S, W, etc. constituting full inversion.

2.3 Analysis of Conduction

Most of the literature on multiphase rectifiers and inverters[5 - 9] gives the analyses of these as applicable to power conversion and suffers from several limiting assumptions. The rectifier and inverter currents are computed according to an assumed constant supply voltage and the current patterns are assumed nearly rectangular as in Fig. 2.3. The equivalent

circuit developed in reference 7 represents the available equivalent d.c. voltage for inversion and rectification under varying firing angles. In reference 10, the authors have developed the equivalent circuit for a bridge rectifier without any of these assumptions found in references 5 to 9, but the evaluation of the commutation angle is highly involved.

The method adopted for this study of the inverter is the piecewise approach.[10] All the factors affecting the mechanism of inversion are included in the analysis. The method used for the evaluation of commutation angle yields a precise equivalent circuit for the inverter.

Fig. 2.3 indicates the inverter operation with a delay of firing element 1 by β_1 radians from the reference R. β_2 will then be equal to the sum of β_1 and $\pi/3$ radians from the reference R.

For purposes of analysis, the current through element 2 was evaluated and the currents in the other elements under balanced three phase load conditions will have the same waveform displaced only in time. The conduction before the instant I (Fig. 2.3) is assumed to be taking place from R phase through the loop made up of, element 1, d.c. source, element 6, and Y phase (Fig. 2.2). This assumption makes the analysis valid only for continuous steady state operation of the inverter. Fig. 2.4 indicates the circuit conditions prior to instant I.

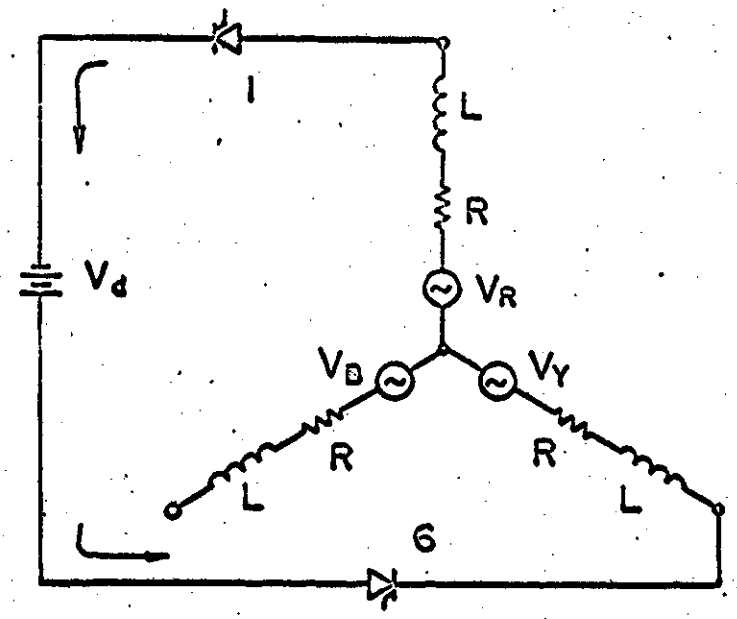

Figure 2.4: Circuit Conditions prior to Interval 1.

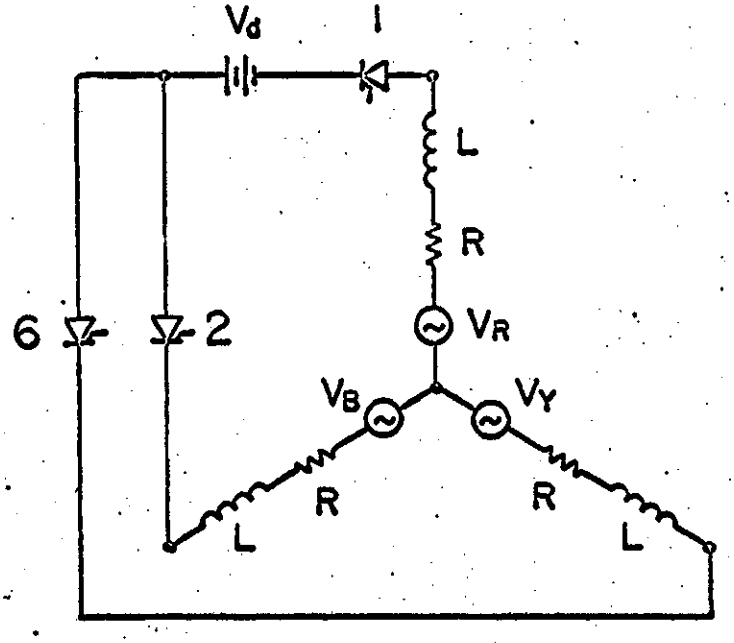

Figure 2.5: Circuit Conditions During Interval 1.

2.4 Conduction Equations

The conduction process during inversion can be divided into five definite intervals.

2.4.1 Interval 1

Interval 1 starts from I when 2 is fired and lasts for γ radians until the change over of current on commutation from element 6 to 2 is complete. It ends when element 6 switches off. The circuit configuration will be as shown in Fig. 2.5. The following conduction equations apply.

$$V_R - I_1 (pL + R) + I_6 (pL + R) - V_Y + Vd = 0 \quad (2.1)$$

$$V_R - I_1 (pL + R) + I_2 (pL + R) - V_B + Vd = 0 \quad (2.2)$$

$$I_1 + I_2 + I_6 = 0 \quad (2.3)$$

Eliminating I_1 and I_6 from the equations and solving for I_2, the following solution for I_2 during interval 1 will result. (Appendix 7.2)

$$I_{2(1)} = C_1 \epsilon^{-Rt/L} - \frac{Vd}{3R} + \frac{Vm}{Z}\left[K_1 \mathrm{Sin}(\omega t - \phi) - K_2 \mathrm{Cos}(\omega t - \phi)\right] \quad (2.4)$$

where

$$K_1 = \frac{-3\sqrt{3}\mathrm{Cos}\beta_2 - 3\mathrm{Sin}\beta_2}{6} \quad (2.5)$$

$$K_2 = \frac{3\sqrt{3}\mathrm{Sin}\beta_2 - 3\mathrm{Cos}\beta_2}{6} \quad (2.6)$$

The time is reckoned from instant I for these equations and hence:

$$I_{2(1)} = 0 \text{ when } t = 0.$$

Therefore:

$$C_1 = \frac{Vd}{3R} + \frac{Vm}{Z}(K_1 \text{Sin}\phi + K_2 \text{Cos}\phi) \qquad (2.7)$$

At t = 0, when 2 is fired, current in 6 decreases which can be seen by obtaining an expression for I_6 from equations (2.1), (2.2) and (2.3) and noting that dI_6/dt is positive for the delay angles of inverter operation (expression for I_2 is negative because of conventions adopted). Similarly it can be seen that the current in element 2 increases from the instant it is fired. This establishes the validity of the circuit as shown in Fig. 2.5 for interval 1.

2.4.2 Interval 2

After element 6 is switched off the interval 2 starts and lasts until element 3 is fired. Element 3 will be fired after 60° from the start of interval 1 and, therefore, it is necessary that γ be less than 60°. The circuit configuration during interval 2 will be as shown in Fig. 2.6. The following conduction equations apply.

$$V_R - I_1 (pL + R) + Vd + I_2 (pL + R) - V_B = 0 \qquad (2.8)$$

$$I_1 + I_2 = 0 \qquad (2.9)$$

The solution for I_2 is (Appendix 7.2),

$$I_{2(2)} = C_2 \epsilon^{-Rt/L} - \frac{Vm}{Z}\left[K_3 \text{Sin}(\omega t - \phi) + K_4 \text{Cos}(\omega t - \phi)\right] - \frac{Vd}{2R} \qquad (2.10)$$

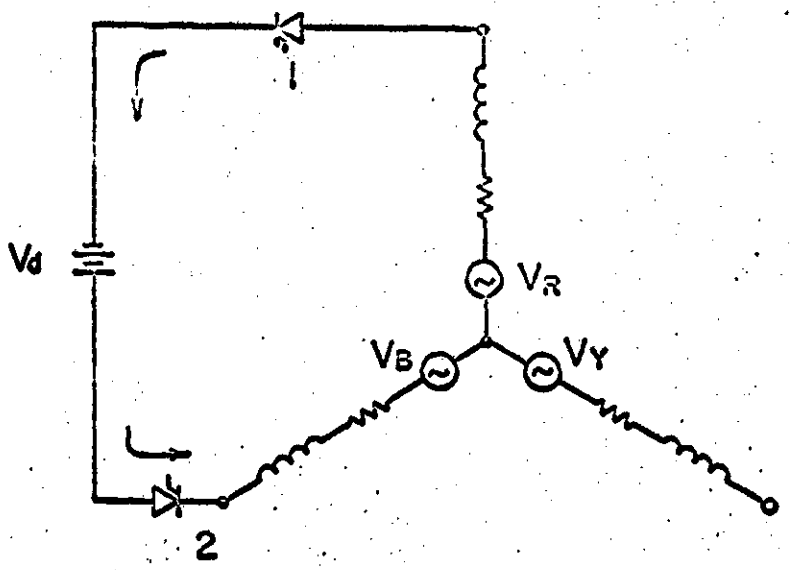

Figure 2.6: Circuit Conditions During Interval 2.

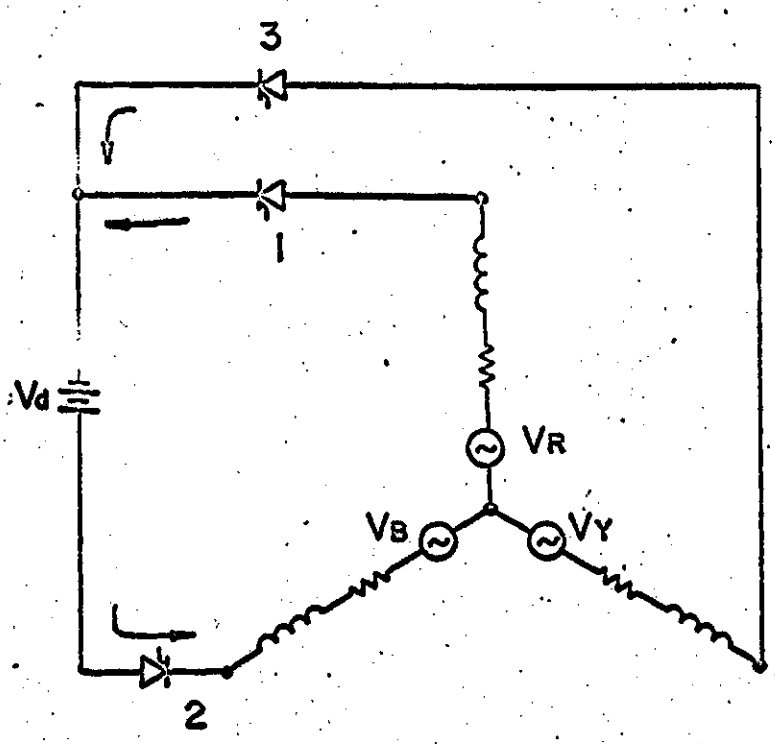

Figure 2.7: Circuit Conditions During Interval 3.

where

$$K_3 = \frac{\sqrt{3}\cos(\beta_2 + \gamma)}{2} \qquad (2.11)$$

$$K_4 = \frac{\sqrt{3}\sin(\beta_2 + \gamma)}{2} \qquad (2.12)$$

the time being reckoned from the start of interval 2.

At $t = 0$

$$I_{2(2)}\Big|_{t=0} = I_{2(1)} \qquad (2.13)$$

Therefore,

$$C_2 = I_{2(1)} - \frac{Vm}{Z}(K_3\sin\phi - K_4\cos\phi) + \frac{Vd}{2R} \qquad (2.14)$$

2.4.3 Interval 3

After a time interval of $\pi/3\omega$ seconds from the start of interval 1, element 3 is fired. The circuit configuration will be as shown in Fig. 2.7. By the same reasoning as applied to interval 1, it can be established that the current in element 3 decreases and that in 1 increases during inversion. The a.c. source has balanced voltages and impedances; therefore, the time taken by the current in 3 to grow to full value is the same as the time taken by the current in element 1 to fall to zero which is the same as the time taken by current in element 6 to decay to zero during interval 1. Hence, the duration of interval 3 is γ radians. The circuit configuration will be as shown in Fig. 2.7. The following conduction equations apply.

$$V_R - I_1 (pL + R) + V_d + I_2 (pL + R) - V_B = 0 \quad (2.15)$$

$$V_Y - I_3 (pL + R) + I_2 (pL + R) - V_B + V_d = 0 \quad (2.16)$$

$$I_1 + I_2 + I_3 = 0 \quad (2.17)$$

The solution for current during interval 3 is (Appendix 7.2):

$$I_{2(3)} = C_3 \epsilon^{-Rt/L} + \frac{Vm}{Z}\left[K_5 \mathrm{Sin}(\omega t - \phi) - K_6 \mathrm{Cos}(\omega t - \phi)\right] - \frac{2Vd}{3R} \quad (2.18)$$

where

$$K_5 = \frac{-3\sqrt{3}\mathrm{Cos}\beta_2 - 3\mathrm{Sin}\beta_2}{6} \quad (2.19)$$

$$K_6 = \frac{3\mathrm{Cos}\beta_2 + 3\sqrt{3}\mathrm{Sin}\beta_2}{6} \quad (2.20)$$

time being reckoned from the start of interval 3.

At $t = 0$,

$$I_{2(3)}\Big|_{t=0} = I_{2(2)}\, e$$

Therefore,

$$C_3 = I_{2(2)}\, e + \frac{Vm}{Z}(K_5 \mathrm{Sin}\phi + K_6 \mathrm{Cos}\phi) + \frac{2Vd}{3R} \quad (2.21)$$

2.4.4 Interval 4

Interval 4 starts after an angle of $[\pi/3]+\gamma$ radians from the start of interval 1 and lasts for $[\pi/3]-\gamma$ radians until 4 is fired. The circuit configuration will be as shown in Fig. 2.8. The conduction equations for this interval are:

$$-V_B + V_Y - I_3 (pL + R) + V_d + I_2 (pL + R) = 0 \quad (2.22)$$

$$I_3 + I_2 = 0 \quad (2.23)$$

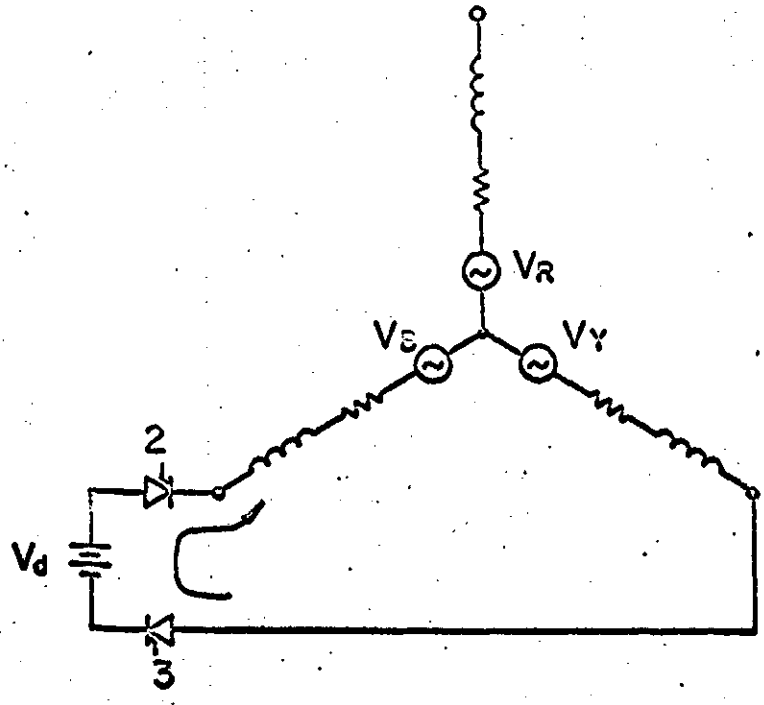

Figure 2·8 : Circuit Conditions During Interval 4·

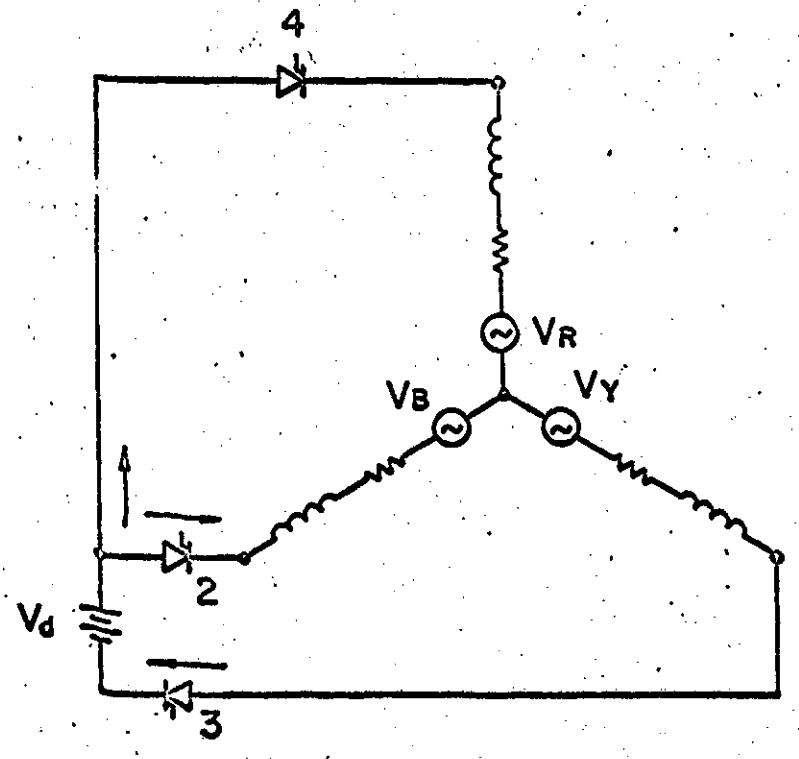

Figure 2·9 : Circuit Conditions During Interval 5.

The solution for I_2 during interval 4 is (Appendix 7.2)

$$I_{2(4)} = C_4\epsilon^{-Rt/L} - \frac{Vm}{Z}\left[K_7\mathrm{Sin}(\omega t-\phi) + K_8\mathrm{Cos}(\omega t-\phi)\right] - \frac{Vd}{2R} \quad (2.24)$$

where

$$K_7 = \frac{\sqrt{3}\mathrm{Cos}(\beta_2 + \gamma)}{2} \quad (2.25)$$

$$K_8 = \frac{\sqrt{3}\mathrm{Sin}(\beta_2 + \gamma)}{2} \quad (2.26)$$

time being reckoned from the start of interval 4.
At $t = 0$,

$$I_{2(4)}\Big|_{t=0} = I_{2(3)}\ e$$

Therefore,

$$C_4 = I_{2(3)}\ e + \frac{Vm}{Z}(K_8\mathrm{Cos}\phi - K_7\mathrm{Sin}\phi) + \frac{Vd}{2R} \quad (2.27)$$

2.4.5 Interval 5

Interval 5 starts when 4 is fired. For the present, it is assumed that the current in element 2 starts to decrease while in 4 it is assumed to increase. By symmetry, the current in element 2 should reach a value of zero to turn it off after γ radians. The circuit configuration will be as shown in Fig. 2.9 and the conduction equations will be:

$$V_Y - I_3\ (pL + R) + V_d + I_2\ (pL + R) - V_B = 0 \quad (2.28)$$

$$V_Y - I_3\ (pL + R) + V_d + I_4\ (pL + R) - V_R = 0 \quad (2.29)$$

$$I_2 + I_3 + I_4 = 0 \quad (2.30)$$

The solution for I_2 during interval 5 is (Appendix 7.2):

$$I_{2(5)} = C_5\epsilon^{-Rt/L} + \frac{Vm}{Z}\left[K_9\mathrm{Sin}(\omega t-\phi) - K_{10}\mathrm{Cos}(\omega t-\phi)\right] - \frac{Vd}{3R} \quad (2.31)$$

where

$$K_9 = \mathrm{Sin}\beta_2 \quad (2.32)$$

$$K_{10} = \mathrm{Cos}\beta_2 \quad (2.33)$$

time being reckoned from the start of interval 5.

At $t = 0$,

$$I_{2(5)}\Big|_{t=0} = I_{2(4)}\ e$$

Therefore,

$$C_5 = I_{2(4)}\ e + \frac{Vm}{Z}(K_9\mathrm{Sin}\phi + K_{10}\mathrm{Cos}\phi) + \frac{Vd}{3R} \quad (2.34)$$

The conduction equations and intervals are summarized in Table 2.1.

2.5 Solution of Conduction Equations

The equations in Table 2.1 representing conduction for the different intervals can be solved if the commutation angle γ is known. The commutation angle depends on the value of the current and, therefore, there is no explicit method of determining γ and hence, the different interval equations cannot be determined discretely. The equations can be solved on a digital computer by a process of iterations. A program was written to solve these equations using a digital computer. Initially, a value of γ is assumed, the equations are solved and the current at the end of interval 5 is evaluated. If the correct value of γ has been assumed, the current at the

Interval	Conduction Period	Duration	Conduction Equations
1	$\frac{\pi}{6}+\beta_2$ to $\frac{\pi}{6}+\beta_2+\gamma$	γ	$I_{2(1)} = C_1\epsilon^{-Rt/L} + V_m/Z[K_1\sin(\omega t-\phi) - K_2\cos(\omega t-\phi)] - \frac{Va}{3R}$ $C_1 = \frac{Vm}{Z}(K_1\sin\phi + K_2\cos\phi) + \frac{Vd}{3R}$ $K_1 = (-3\sqrt{3}\cos\beta_2 - 3\sin\beta_2)/6;\ K_2 = (3\sqrt{3}\sin\beta_2 - 3\cos\beta_2)/6$
2	$\frac{\pi}{6}+\beta_2+\gamma$ to $\beta_2+\frac{\pi}{2}$	$\frac{\pi}{3}-\gamma$	$I_{2(2)} = C_2\epsilon^{-Rt/L} - \frac{Vm}{Z}[K_3\sin(\omega t-\phi) + K_4\cos(\omega t-\phi)] - \frac{Va}{2R}$ $C_2 = I_{2(1)e} - \frac{Vm}{Z}(K_3\sin\phi - K_4\cos\phi) + \frac{Vd}{2R}$ $K_3 = [\sqrt{3}\cos(\beta_2+\gamma)]/2;\ K_4 = [\sqrt{3}\sin(\beta_2+\gamma)]/2$
3	$\beta_2+\frac{\pi}{6}$ to $\beta_2+\frac{\pi}{6}+\gamma$	γ	$I_{2(3)} = C_3\epsilon^{-Rt/L} + \frac{Vm}{Z}[K_5\sin(\omega t-\phi) - K_6\cos(\omega t-\phi)] - \frac{2Vd}{3R}$ $C_3 = I_{2(2)e} + \frac{Vm}{Z}(K_5\sin\phi + K_6\cos\phi) + \frac{2Vd}{3R}$ $K_5 = (-3\sqrt{3}\cos\beta_2 - 3\sin\beta_2)/6;\ K_6 = (3\cos\beta_2 + 3\sqrt{3}\sin\beta_2)/6$
4	$\beta_2+\frac{\pi}{6}+\gamma$ to $\beta_2+\frac{\pi}{6}$	$\frac{\pi}{3}-\gamma$	$I_{2(4)} = C_4\epsilon^{-Rt/L} - \frac{Vm}{Z}[K_7\sin(\omega t-\phi) + K_8\cos(\omega t-\phi)] - \frac{Vd}{2R}$ $C_4 = I_{2(3)e} + \frac{Vm}{Z}(K_8\cos\phi - K_7\sin\phi) + \frac{Vd}{2R}$ $K_7 = [\sqrt{3}\cos(\beta_2+\gamma)]/2;\ K_8 = [\sqrt{3}\sin(\beta_2+\gamma)]/2$
5	$\beta_2+\frac{5\pi}{6}$ to $\beta_2+\frac{5\pi}{6}+\gamma$	γ	$I_{2(5)} = C_5\epsilon^{-Rt/L} + \frac{Vm}{Z}[K_9\sin(\omega t-\phi) - K_{10}\cos(\omega t-\phi)] - \frac{Vd}{3R}$ $C_5 = I_{2(4)e} + \frac{Vm}{Z}(K_9\sin\phi + K_{10}\cos\phi) + \frac{Vd}{3R}$ $K_9 = \sin\beta_2;\ K_{10} = \cos\beta_2$

Table 2.1 Summary of Conduction Equations

end of interval 5 will be zero. If the current is not zero at the end of interval 5, the value of γ is successively incremented by small values and the calculations are repeated until the current at the end of interval 5 is found to be zero.

The duration of the five different intervals can be determined after the value of γ is found and, hence, the conduction pattern in element 2 over half a cycle can be determined. During the other half period of the a.c. voltage wave, element 2 cannot conduct current but element 5, which is connected to the same phase as element 2, conducts current. The current pattern in element 5 will be exactly similar to that of element 2 and, hence, the conduction pattern in phase B over a complete cycle can be determined.

The Fortran IV program written for the solution of the conduction equations using an IBM 7040 computer is discussed in Appendix 7.3.

2.6 The Equivalent Circuit

The wave form of the current through an element and, hence, the Fourier series representation of the current is a function of the combined effects of the a.c. and the d.c. sources and of the firing angle; therefore, the equivalent circuit consists only of the harmonic generators representing the Fourier coefficients of the elementary currents. The equivalent circuit of one phase of the inverter is shown in Fig. 2.11.

2.7 Analysis of Conduction Equations

The equivalent circuit developed is for conditions of conduction over half a cycle of the voltage wave. Discontinuous conduction can occur at low d.c. voltages when the inversion currents flow in pulses through the elements over half a cycle of the voltage wave. The conduction equations developed are not valid for cases of discontinuous conduction.

Solid lines in Fig. 2.10 indicate the circuit configuration immediately before element 2 is fired. When element 2 is fired, interval 1 starts and the broken lines in Fig. 2.10 indicate the additions to the circuit which come into action. If conduction is to start in element 2, the d.c. voltage must be greater than the opposing voltage in the loop a'-c-o-a (Fig. 2.10). Equation (2.35) specifies this condition

$$V_d = V_B\Big|_{t=\frac{\pi}{6}+\beta_2-\frac{4\pi}{3}} \pm L\frac{dI_6}{dt} + RI_6 + V_R\Big|_{t=\frac{\pi}{6}+\beta_2} \qquad (2.35)$$

The sign of $L(dI_6/dt)$ cannot be assigned at the outset; however, from the conduction pattern obtained for element 2, it is found that I_2 at the end of interval 4 is decreasing. Due to symmetrical conditions assumed, I_6 at the start of interval 1 is the same as I_2 at the end of interval 4. The value of I_6, as of any other elementary current, being dependent on V_d, equation 2.35 cannot uniquely determine the value of V_d for inversion.

An examination of equations for interval 5 reveals that the current during interval 5, as in any other interval, is composed of three components: the d.c. component of

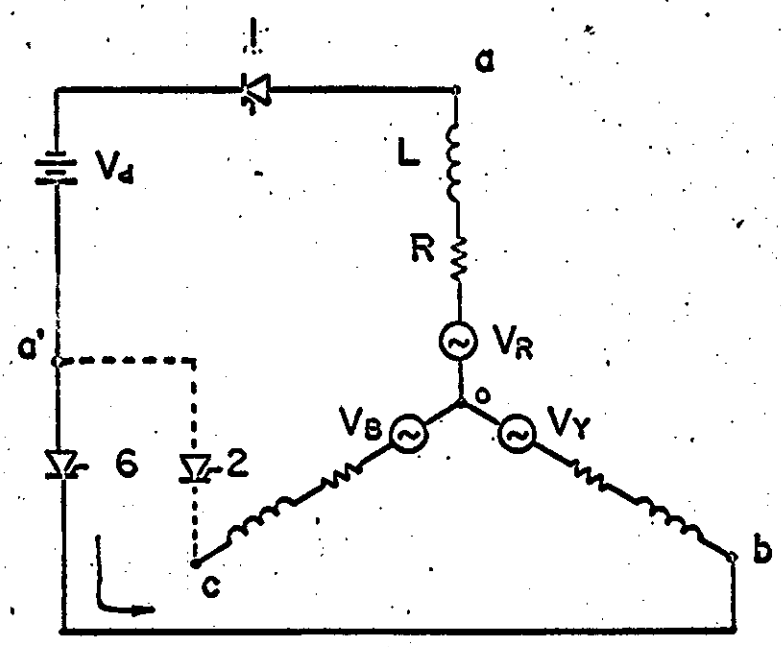

Figure 2·10 Circuit Conditions at the Instant of Switching Element 2·

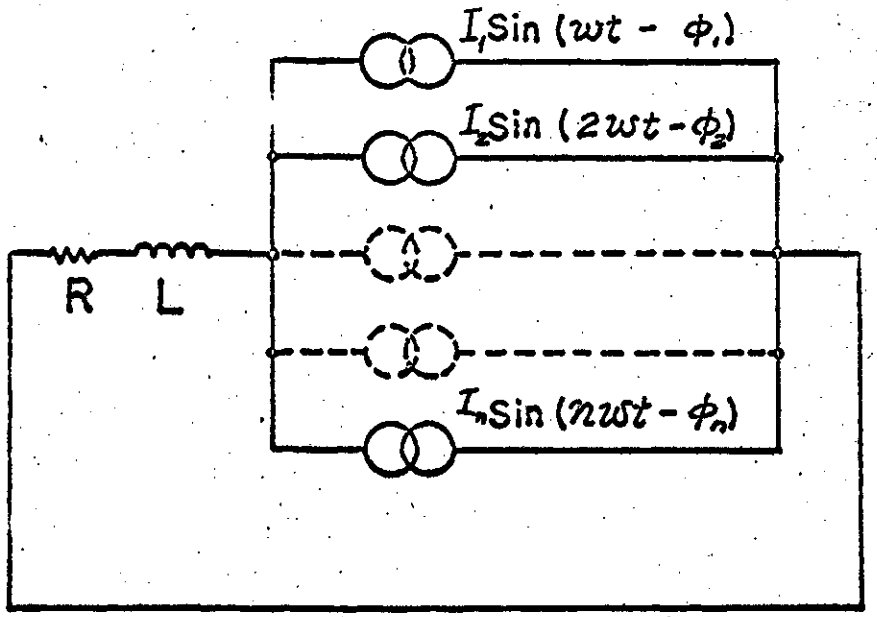

Figure 2-11: Equivalent Circuit of a Bridge Inverter

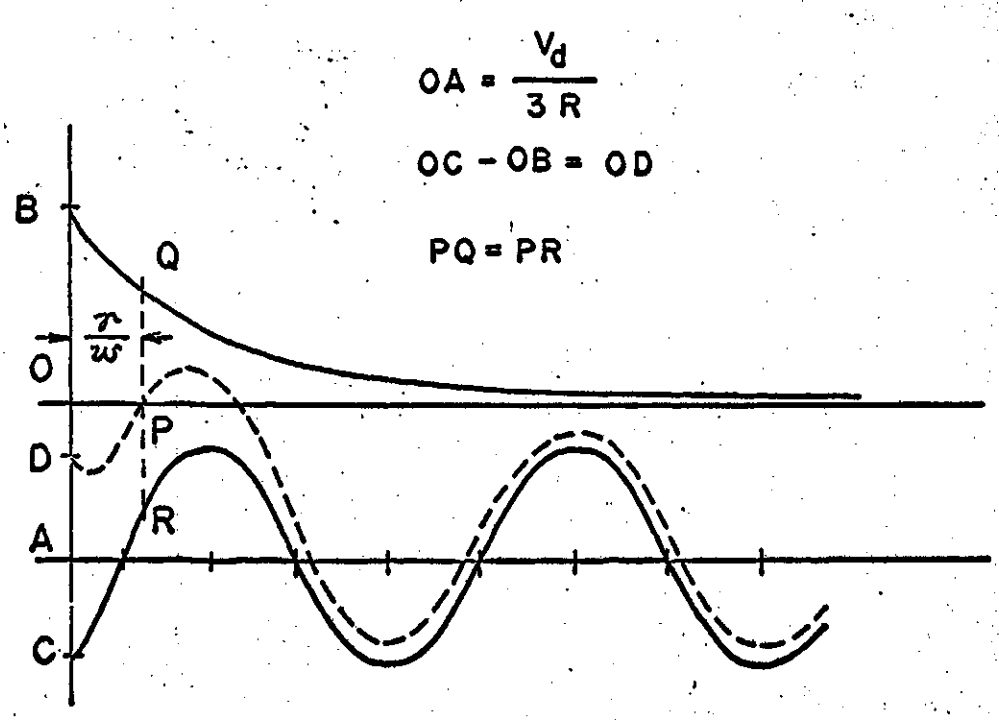

Figure 2-12 : Component Currents of Intervals

magnitude $V_d/3R$, the a.c. component and an exponentially decaying component. The time constant of the exponentially decaying component is equal to the L/R ratio of the a.c. source impedance. Fig. 2.12 indicates these component currents. The current in element 2 decays to zero after γ/ω seconds. This can be seen by the resultant current shown dotted in the figure. Thus, it can be established that the commutation angle is dependent on the L/R ratio of the a.c. source impedance and the d.c. and the a.c. voltages. The digital computer program written for the solution of γ gives these components of current as output for different values of d.c. voltages, a.c. voltages and the resistances and inductances of the a.c. source.

The equivalent circuit developed for the inverter is a powerful tool for the analysis of systems of which they are a part. The calculation of the elementary currents is the basic step in the analysis of the high voltage a.c. d.c. links, communication interference of HVDC links, motor torques and other such effects observable in the circuits with rectifiers or inverters as their components. The conduction equations offer a better insight into the mechanism of inversion. A particular application of the equivalent circuit in the analysis of the torque of induction motors is presented in the following chapter.

3. THE INVERTER IN THE ROTOR OF A THREE PHASE INDUCTION MOTOR

3.1 Generalized Equations of an Induction Motor

3.1.1 The circuit for analysis

The three phase induction motor has three sets of windings on its stator and three sets of windings on its rotor, i.e. one set on each phase. The rotor and the stator may be connected in star or in delta. The phases of the stator are brought out to the terminals and the rotor phases are connected to three slip rings. The performance analysis which follows is based on the assumption that the stator and the rotor are star connected; any delta connected machine must be transformed to its equivalent star before this analysis can be applied.

The stator phase windings have mutual inductances with corresponding phases in the rotor. These mutual inductances are functions of the instantaneous rotor position. Fluxes which link only the individual phase windings contribute to leakage reactances which are independent of rotor position.

The exact analysis of the effect of the leakage inductances and the paths of leakage fluxes is very complex in nature and the contributing factors for these have been discussed in books on machine theory.[11,12]

It has been established[11,12] that the induction motor can be represented to a reasonable degree of accuracy,

for steady state analysis, by its single phase equivalent circuit as shown in Fig. 3.1. The values indicated in the figure are on a per phase basis, R and X representing the resistance and the leakage reactance of the phase winding and X_ϕ the magnetizing impedance, per phase of stator wye.

If a three phase inverter is connected to the rotor, part of the energy input into the rotor from the inverter is given out as mechanical power and a part of the energy is transferred across the air gap to the stator windings and returned to the a.c. supply mains. The leakage impedances of the induction motor are usually considerably larger in magnitude than the impedances of the power sources to which it is connected; hence, if viewed from the rotor, the stator can be considered as a winding which is connected to an emf source of zero internal impedance. The conditions existing for inversion can, therefore, be represented as in Fig. 3.2.

Before an analysis of the circuit of Fig. 3.2 can be undertaken, the equivalent circuit of the inverter under conditions of inversion into the rotor must be established. The approach suggested in Chapter 2 can be adopted to establish this equivalent circuit provided that the induction motor can be represented by an equivalent circuit similar to that of the a.c. source in Chapter 2. The inductances of an induction motor are very complex in nature due to the relative motion between the rotor and the stator windings; consequently, an exact analysis of the inversion currents is highly

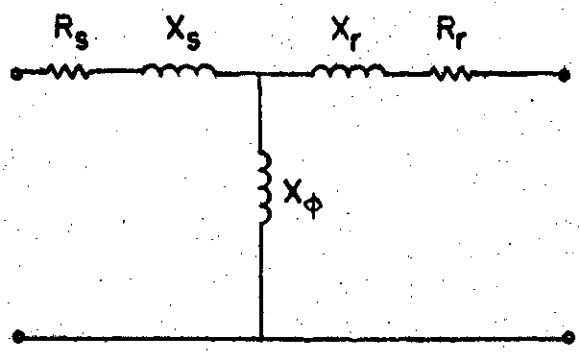

Figure 3-1: Equivalent Circuit of Motor

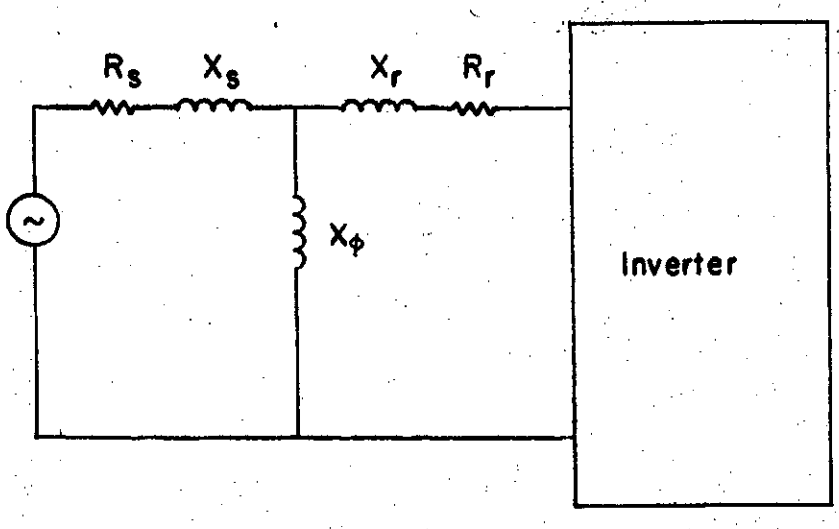

Figure 3-2: Equivalent Circuit with Inverter in the Rotor

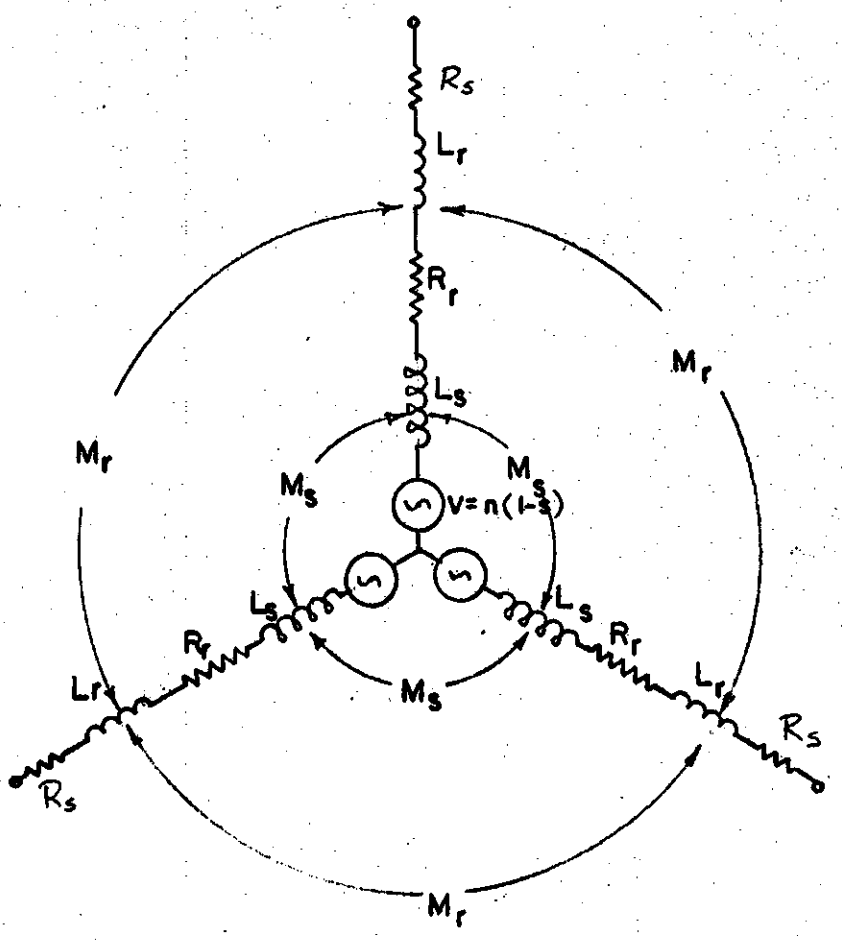

FIGURE 3.3: *EQUIVALENT CIRCUIT OF MOTOR — alternative form.*

complicated. To simplify matters, approximations are made to yield the inversion currents to a reasonable degree of accuracy.

If constant air gap magnetic flux is assumed (this assumption has the effect of shifting the magnetizing impedance X_ϕ in Fig. 3.1 to the extreme left), and that all the flux produced by the stator coils link the rotor, the motor can be represented by an equivalent circuit as shown in Fig. 3.3. Each phase in Fig. 3.3 contains a voltage source of value $V_s n(1-s)$ where V_s is the stator voltage, s the slip of the induction motor and n the ratio of stator to rotor turns per phase. The sum of the stator and the rotor leakage impedances are included in series with the voltage source.

The mutual couplings between stator phases due to flux which does not cross the air gap can be shown to be small[11,12] and were assumed to be zero in this analysis. The same approximation applies to the interphase couplings between the rotor phases. The mutual inductance M_s and M_r in Fig. 3.3 can therefore be neglected and the equivalent circuit of the induction motor reduces to that of the a.c. source described in Chapter 2.

The representation of the induction motor by the equivalent circuit shown in Fig. 3.2 is not satisfactory for the calculation of torque and power relations if the rotor currents contain harmonics. A more convenient representation for such analyses is the two axes generalized equivalent machine.

3.1.2 Induction motor as a generalized machine

It has been shown by the authors in references 11, 13, 14 and 15 that the 3 phase induction machine can be transformed to a machine of the type shown in Fig. 3.4. The generalized machine in Fig. 3.4 has two axes of symmetry (the axis of symmetry is generally chosen to coincide with the symmetry of the magnetic circuit; the induction motor being a cylindrical rotor machine, can be represented on any arbitrarily chosen axes) and the rotor and the stator have a coil in each of the axes. In Fig. 3.4, the reference axes, called direct and quadrature axes, are stationary and the rotor is revolving with an angular velocity v.

Fig. 3.5 indicates another form of a generalized machine to which the induction motor can be transformed. The d and q axes of the stator together with their coils are revolving synchronously at an angular velocity ω. The rotor mmfs resolved along these two axes are equivalent to those produced by the coils on the d and q axes in the equivalent machine. The rotor is revolving at an angular velocity v. OA and OB in Fig. 3.5 are the axes of the rotor. If θ_s is the angle between the stator and the rotor axes at any instant, the operation of the induction motor can be described by the following equations.*(12,13,14)

---

* The matrix notation used agrees with references 12, 13 and 14.

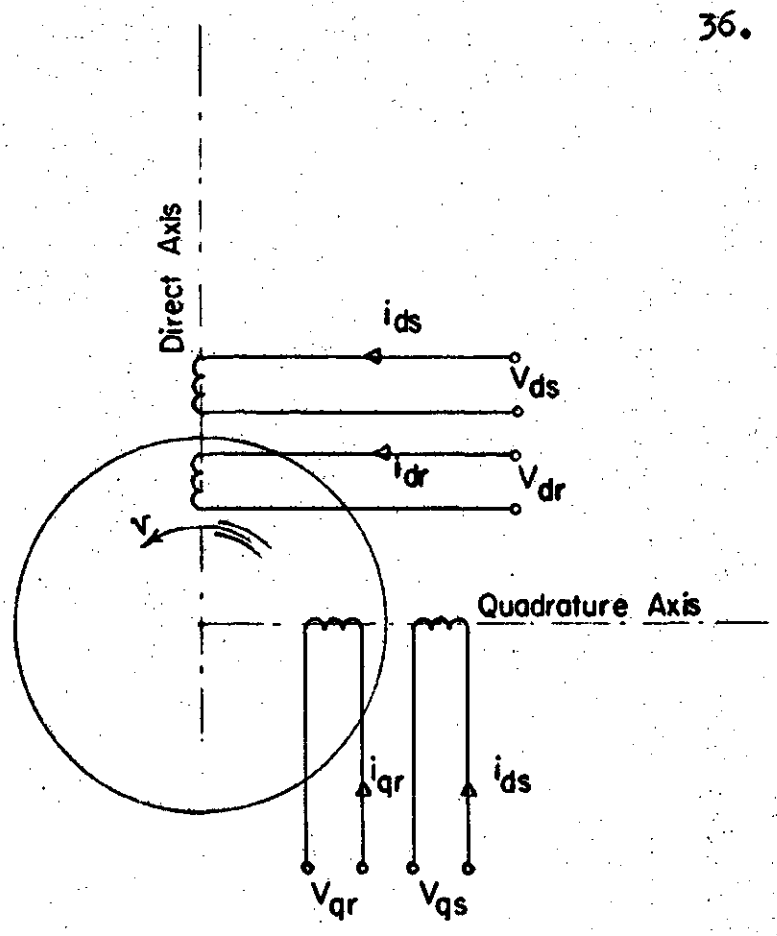

Figure 3.4: Generalised Machine - fixed reference axes

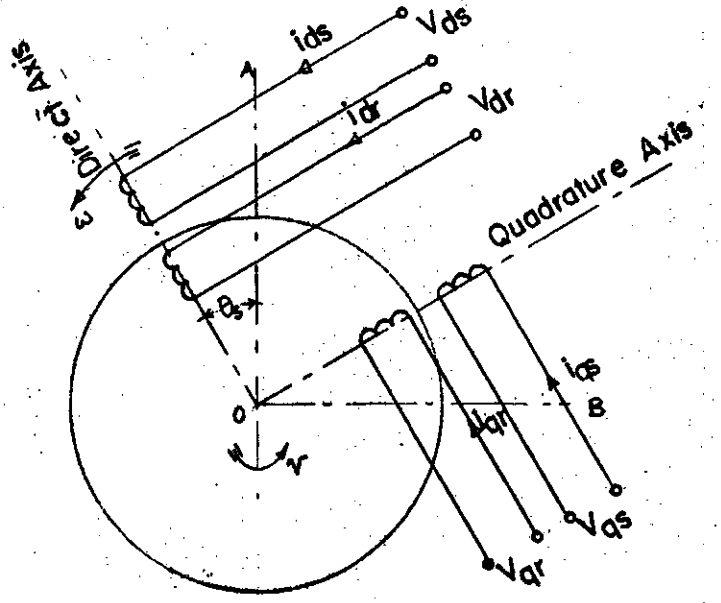

Figure 3.5: Generalised Machine - rotating reference axes

$$\begin{array}{|c|} V_{ds} \\ V_{dr} \\ V_{qr} \\ V_{qs} \end{array} = \begin{array}{c|cccc} & ds & dr & qr & qs \\ ds & R_1+pL_1 & pM & -\omega M & -\omega L_1 \\ dr & pM & R_2+pL_2 & -p\theta_s L_2 & -p\theta_s M \\ qr & p\theta_s M & p\theta_s L_2 & R_2+pL_2 & pM \\ qs & \omega L_1 & \omega M & pM & R_1+pL_1 \end{array} \cdot \begin{array}{|c|} i_{ds} \\ i_{dr} \\ i_{qr} \\ i_{qs} \end{array} \qquad (3.1)$$

In equations (3.1), L_1 and R_1 are the inductance and resistance of the coils on the stator and L_2 and R_2 the values for the rotor coils of the machine in Fig. 3.5. M is the mutual inductance between the stator and the rotor coils of the generalized machine. It can be established[11] that the value of L_1 is the difference between the stator leakage inductance and the magnetizing inductance, and L_2 is the difference between the rotor leakage inductance and the magnetizing inductance. The mutual inductance M is the same as the magnetizing inductance of the motor.[11] The values of L_1, L_2 and M can, therefore, be determined from the open circuit and the lock rotor tests of the induction motor.

The currents in equation (3.1) are related to the phase currents of the three phase motor by the transformation tensor [Z]

$$[Z] = K \begin{array}{c|ccc} & i_A & i_B & i_C \\ ds & \cos \omega t & \cos(\omega t-120^\circ) & \cos(\omega t+120^\circ) \\ dr & \cos \theta_s & \cos(\theta_s-120^\circ) & \cos(\theta_s+120^\circ) \\ qr & -\sin \theta_s & -\sin(\theta_s-120^\circ) & -\sin(\theta_s+120^\circ) \\ qs & -\sin \omega t & -\sin(\omega t-120^\circ) & -\sin(\omega t+120^\circ) \end{array} \qquad (3.2)$$

where K is a constant.

The analysis of the induction motor torque will be restricted to steady state conditions. Under these conditions, the fundamental frequency components of the rotor and the stator phase currents when transformed to d and q axes appear as d.c. quantities; therefore, terms with coefficients p (where $p = d/dt$) will all be zero for the fundamental components under steady state conditions. Further, under these conditions, the rotor will be revolving at constant speed and will be slipping behind the synchronously rotating d and q axes at a velocity $s\omega$.

3.2 Generalized Equations Applied to Motor with the Inverter in the Rotor

It has been established in Section 3.1.1 that the induction motor can be represented approximately by an equivalent circuit as shown in Fig. 3.3. Using the techniques developed in Chapter 2, the conduction pattern and, hence, the phase current pattern of the rotor coils of the motor can be established. Due to assumed balanced conduction, the fundamental component of the three phase currents in the rotor phases will be displaced by 120 electrical degrees and the nth harmonic component by 120n degrees. The magnitude and the phase relationships of the various harmonic currents in the rotor phases of the actual machine can be obtained by a Fourier analysis of the conduction pattern during inversion. Let the general term of the harmonic current in the rotor phase R be represented by

$$I_{rR} = \sum_{n=1}^{n=\infty} I_n \sin(ns\omega t - \phi_n) \qquad (3.3)$$

where I_n is the magnitude of the nth harmonic current and ϕ_n the phase relationship of the nth harmonic current with reference to the phase voltage. Similarly, the currents in phases Y and B of the rotor can be represented by,

$$I_{rY} = \sum_{n=1}^{n=\infty} I_n \sin(ns\omega t - 120n - \phi_n) \qquad (3.4)$$

$$I_{rB} = \sum_{n=1}^{n=\infty} I_n \sin(ns\omega t + 120n - \phi_n) \qquad (3.5)$$

Under steady state operating conditions, $p\theta_s (p = \frac{d}{dt})$ in equations (3.1) and (3.2) will be equal to $s\omega$, where ω is the synchronous angular velocity and s is the slip of the motor. If this relationship is used in equation (3.2), the harmonic currents of the rotor phase transform to the d and q axis according to the relation (Appendix 7.7)

$$\begin{vmatrix} i_{dr} \\ -i_{qr} \end{vmatrix} = \sum_{n=1}^{n=\infty} \frac{KI_n}{2} \begin{vmatrix} \sin[(n+1)s\omega t - \phi_n] & \sin[(n-1)s\omega t - \phi_n] \\ -\cos[(n+1)s\omega t - \phi_n] & \cos[(n-1)s\omega t - \phi_n] \end{vmatrix} \begin{vmatrix} 2\cos[(n+1)\frac{2\pi}{3}] + 1 \\ 2\cos[(n-1)\frac{2\pi}{3}] + 1 \end{vmatrix} \qquad (3.6)$$

From the analysis of the conduction pattern, it will be shown in Chapter 4 that the conduction pattern has half wave symmetry and, therefore, only odd harmonics flow in the rotor phases. In equation (3.6), n is, therefore, an odd number.

A close analysis of equation (3.6) reveals that the various harmonic currents when transformed to their d and q axes currents appear as,

Fundamental: d.c. current

3^{rd} harmonic: zero

5^{th} harmonic: currents at 6 times the frequency of the fundamental

7^{th} harmonic: currents at 6 times the frequency of the fundamental

9^{th} harmonic: zero

If one considers the rotor currents up to the 9^{th} harmonic, the rotor phase currents are given by,

$$I_{rA} = I_1\sin(s\omega t-\phi_1) + I_3\sin(3s\omega t-\phi_3) + I_5\sin(5s\omega t-\phi_5) + I_7\sin(7s\omega t-\phi_7) + I_9\sin(9s\omega t-\phi_9) \qquad (3.7)$$

The transformation of the phase currents to d and q axes currents using the relation given by (3.6) gives the d and q currents in the rotor as,

$$i_{dr} = K[1.5I_1\sin(-\phi_1) + 1.5I_5\sin(6s\omega t-\phi_5) + 1.5I_7\sin(6s\omega t-\phi_7)] \quad (3.8)$$

and

$$-i_{qr} = K[1.5I_1\cos(-\phi_1) - 1.5I_5\cos(6s\omega t-\phi_5) + 1.5I_7\cos(6s\omega t-\phi_7)] \quad (3.9)$$

The value of the constant K is the same as in equations (3.2) and (3.6). The constant K has been evaluated as 0.4714 for the laboratory machine in Appendix 7.4.

3.3 Torque Calculations

Equation (3.1) describes the operation of the induction motor. The values of V_{ds} and V_{qs}, the stator d and q axes voltages, can be found knowing the terminal conditions. The values of i_{dr} and i_{qr}, the rotor d and q currents, can be obtained using equation (3.6) after establishing the conduction pattern. Substituting these known values in the four equations resulting from the matrices of (3.1), the four unknowns, the stator d and q currents and the rotor d and q voltages, can be solved for. For the purposes of torque computations, only the values of the stator d and q currents are necessary. Expanding (3.1) results in equations (3.10) and (3.11) as

$$i_{ds}(R_1+pL_1) + pMi_{dr} - \omega Mi_{qr} - \omega L_1 i_{qs} = V_{ds} \quad (3.10)$$

$$i_{ds}\omega L_1 + i_{dr}\omega M + pMi_{qr} + (R_1+pL_1)i_{qs} = V_{qs} \quad (3.11)$$

The reference position of the d and q axes may be chosen with the d axis perpendicular to the air gap m mf at time t = 0 so that V_{ds} will be equal to zero. Then, equations (3.10) and (3.11) may be written as,

$$i_{ds}(R_1+pL_1) - \omega L_1 i_{qs} = \omega M i_{qr} - pM i_{dr} \qquad (3.12)$$

$$i_{qs}(R_1+pL_1) + \omega L_1 i_{ds} = -\omega M i_{dr} - pM i_{qr} + V_{qs} \qquad (3.13)$$

The multiplication of equation (3.12) by ωL_1 and (3.13) by (R_1+pL_1) results in,

$$i_{ds}(R_1+pL_1)\omega L_1 - \omega^2 L_1^2 i_{qs} = \omega L_1(\omega M i_{qr} - pM i_{dr}) \qquad (3.14)$$

$$i_{ds}(R_1+pL_1)\omega L_1 + i_{qs}(R_1+pL_1)^2 = (R_1+pL_1)(V_{qs} - pM i_{qr} - \omega M i_{dr}) \qquad (3.15)$$

Subtracting (3.14) from (3.15),

$$i_{qs}\left[(R_1+pL_1)^2 + \omega^2 L_1^2\right] = i_{qr} M(-\omega^2 L_1 - R_1 p - p^2 L_1) - \omega M R_1 i_{dr} + V_{qs} R_1 + pL_1 V_{qs} \qquad (3.16)$$

If the applied voltage to the stator is at fundamental frequency, free from harmonics, V_{qs} can be shown to be a d.c. quantity from equation (3.2). Hence, the term $pV_{qs}L_1$ in equation (3.16) has a value equal to zero. The values of i_{qr} and i_{dr} can be obtained from the conduction pattern using the transformation (3.6); therefore, equation (3.16) can be solved to obtain i_{qs} if the parameters of the motor are known. Equation (3.16) is a linear differential equation and can be

solved as shown below.

The currents at a frequency of $6s\omega$ in equations (3.8) and (3.9) can be combined and written as,

$$i_{dr} = K\left[1.5I_1\sin(-\phi_1) + I_{6Rd}\sin(6s\omega t-\phi_{Rd})\right] \qquad (3.17)$$

$$-i_{qr} = K\left[1.5I_1\cos(-\phi_1) + I_{6Rq}\cos(6s\omega t-\phi_{Rq})\right] \qquad (3.18)$$

The symbols I_{6Rd} and ϕ_{Rq} are defined in Fig. 3.6. Solving (3.16) for i_{qs}, since pL_1V_{qs} is zero,

$$i_{qs} = \frac{M(-\omega^2L_1-R_1p-p^2L_1)i_{qr} - \omega MR_1i_{dr} + V_{qs}R_1}{\left[(R_1 + pL_1)^2 + \omega^2L_1^2\right]} \qquad (3.19)$$

Each of the direct and the quadrature axes rotor currents contains a d.c. quantity and an a.c. quantity of angular velocity $6s\omega$. This can be seen from equations (3.17) and (3.18). The substitution of these values of i_{dr} and i_{qr} from equations (3.17) and (3.18) into (3.19) gives

$$i_{qs} = i_{\alpha 1} + i_{\beta 1} \qquad (3.20)$$

where $i_{\alpha 1}$ is a d.c. quantity and $i_{\beta 1}$ is an a.c. quantity of angular velocity $6s\omega$. In Appendix 7.5, it is shown that

$$i_{\alpha 1} = \left[V_{qs}R_1 + 1.5KI_1M(\omega^2L_1\cos\phi_1 - \omega R_1\sin\phi_1)\right]/(R_1^2 + \omega^2L_1^2) \qquad (3.21)$$

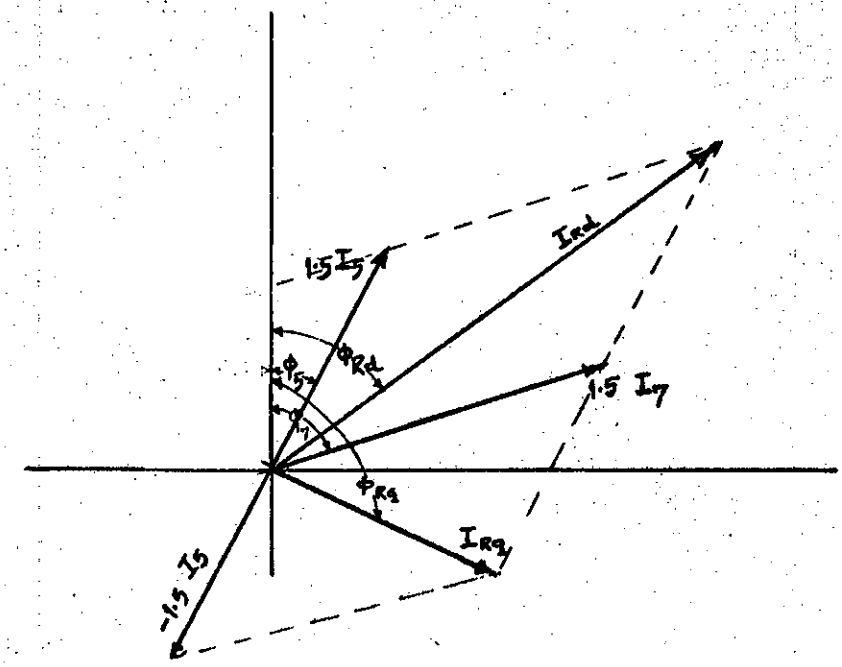

FIGURE 3.6: *VECTORIAL REPRESENTATION OF HARMONIC CURRENTS*

$$i_{\beta 1} = -\frac{K}{Q}\left\{I_{6Rq}M\left[R_1 6s\omega\sin(6s\omega t-\phi_{Rq}-\delta) - \omega^2 L_1\cos(6s\omega t-\phi_{Rq}-\delta)\right.\right.$$
$$\left.\left. + L_1 36s^2\omega^2\cos(6s\omega t-\phi_{Rq}-\delta)\right] + I_{6Rd}\omega MR_1\sin(6s\omega t-\phi_{Rd}-\delta)\right\} \quad (3.22)$$

where the values of Q and δ are,

$$Q = \sqrt{(R_1^2 + \omega^2 L_1^2 - 36s^2\omega^2 L_1^2)^2 + 36L_1^2 R_1^2 s^2\omega^2} \quad (3.23)$$

and

$$\delta = \tan^{-1} 2L_1 R_1 s\omega/(R_1^2 + \omega^2 L_1^2 - 36s^2\omega^2 L_1^2) \quad (3.24)$$

Similarly, multiplication of equation (3.12) by $(R_1 + pL_1)$ and (3.13) by ωL_1 and adding the results, one gets

$$i_{ds}\left[(R_1+pL_1)^2 + \omega^2 L_1^2\right] = i_{dr}M(-pR_1-p^2L_1-\omega^2L_1) + \omega MR_1 i_{qr} + V_{qs}\omega L_1 \quad (3.25)$$

Solving for i_{ds},

$$i_{ds} = \frac{i_{dr}M(-pR_1-p^2L_1-\omega^2L_1) + \omega MR_1 i_{qr} + V_{qs}\omega L_1}{\left[(R_1 + pL_1)^2 + \omega^2 L_1^2\right]} \quad (3.26)$$

The substitution of the values for i_{dr} and i_{qr} from equations (3.17) and (3.18) into (3.26) gives

$$i_{ds} = i_{c2} + i_{\beta 2} \quad (3.27)$$

where i_{c2} is a d.c. quantity and $i_{\beta 2}$ is an a.c. quantity of angular velocity $6s\omega$. In Appendix 7.5, it is shown that

$$i_{c2} = \left[V_{qs}\omega L_1 - 1.5KI_1M(\omega R_1\cos\phi_1 + \omega^2 L_1\sin\phi_1)\right]/(R_1^2+\omega^2L_1^2) \quad (3.28)$$

$$i_2 = -\frac{K}{Q}\Big\{I_{6Rd}M\big[R_1 6s\omega\cos(6s\omega t-\phi_{Rd}-\delta) + L_1 36s^2\omega^2\sin(6s\omega t-\phi_{Rd}-\delta)$$

$$+\omega^2 L_1\sin(6s\omega t-\phi_{Rd}-\delta)\big] + I_{6Rq}\omega M R_1\cos(6s\omega t-\phi_{Rq}-\delta)\Big\} \quad (3.29)$$

where Q and are as defined in equations (3.23) and (3.24).

A digital computer program was written to obtain the direct and quadrature axis stator currents by a summation of the various components of the equations (3.21), (3.22), (3.28) and (3.29). This program evaluates the stator currents at any desired values of slip. Details of the program are listed in Appendix 7.6.

3.4 Torque tensor

The rotor and the stator direct and quadrature axes currents of the generalized machine have been evaluated. It has been established that the torque of the machine is[13,14,15]

$$T = [I]_t[C][I] \quad (3.30)$$

where [I] is the current matrix as on the right hand side of equation 3.1 and the torque tensor C is given by the coefficients of $p\theta_s$ in equation 3.1.

Thus,

$$C = \begin{array}{c|cccc} & d_s & g_s & g_r & d_r \\ \hline d_s & & & & \\ g_s & & & -L_2 & -M \\ g_r & M & L_2 & & \\ d_r & & & & \end{array} \quad (3.31)$$

It is to be noted that the elements of the torque tensor are those which give rise to speed voltages.

If one evaluates torque according to equation 3.30, the resulting power will be,

$$P = \text{Torque} \times \text{speed} \tag{3.32}$$

$$P = T \times s\omega \tag{3.33}$$

Therefore,

$$P = s\omega M(i_{gr}i_{ds} + i_{dr}i_{gs}) \tag{3.34}$$

The power in watts is given per pole pair[15] and the power of the three phase machine is given by

$$P_{3pL\ m/c} = \frac{N}{2} s\omega M(i_{gr}i_{ds} + i_{dr}i_{gs}) \tag{3.35}$$

where $\frac{N}{2}$ is the number of pole pairs. The torque in foot lbs. can be evaluated from equation (3.35). The terms i_{dr}, i_{ds}, i_{qr} and i_{qs} contain d.c. components and sixth harmonic a.c. components as shown in Section 3.3. The contribution to the fundamental torque by the d.c. currents and the harmonic torque by the a.c. currents can be evaluated independently from equation (3.33). The digital computer program written for the calculation of stator currents (Appendix 7.6) is also written with a view towards the calculation of the fundamental and the harmonic torques.

In the following chapter, the experimentally measured values are compared with the theoretically predicted torque values based on the equations developed in this chapter.

4. EXPERIMENTAL INVESTIGATIONS

4.1 Physical Test Setup

The physical system illustrated schematically in Fig. 4.1 was used to carry out tests in the laboratory to substantiate the theoretical findings. In general terms, its operation was as follows.

The direct current motor generator set provided a controlled source of d.c. power to the inverter. The d.c. generator was operated as a separately excited reverse compounded machine in order to limit the short circuit current and thus provide protection for the elements of the inverter in the event of a commutation failure. A fast acting circuit breaker was also connected in series with the d.c. generator for purposes of isolation under high currents.

The stator of the induction motor was connected to the 3 phase a.c. supply mains. The three phase bridge inverter supplied energy to the rotor at the frequency of the rotor voltages. The firing pulses for the control of the inverter was obtained from a firing circuit (details of operation of the firing circuit can be found in Appendix 7.1). The firing circuit was made to deliver the pulses at the rotor frequency through the use of a mechanical differential gear arrangement.

A direct current motor coupled to the induction motor served the purpose of running the induction motor at different speeds. The measurement of the energy input to

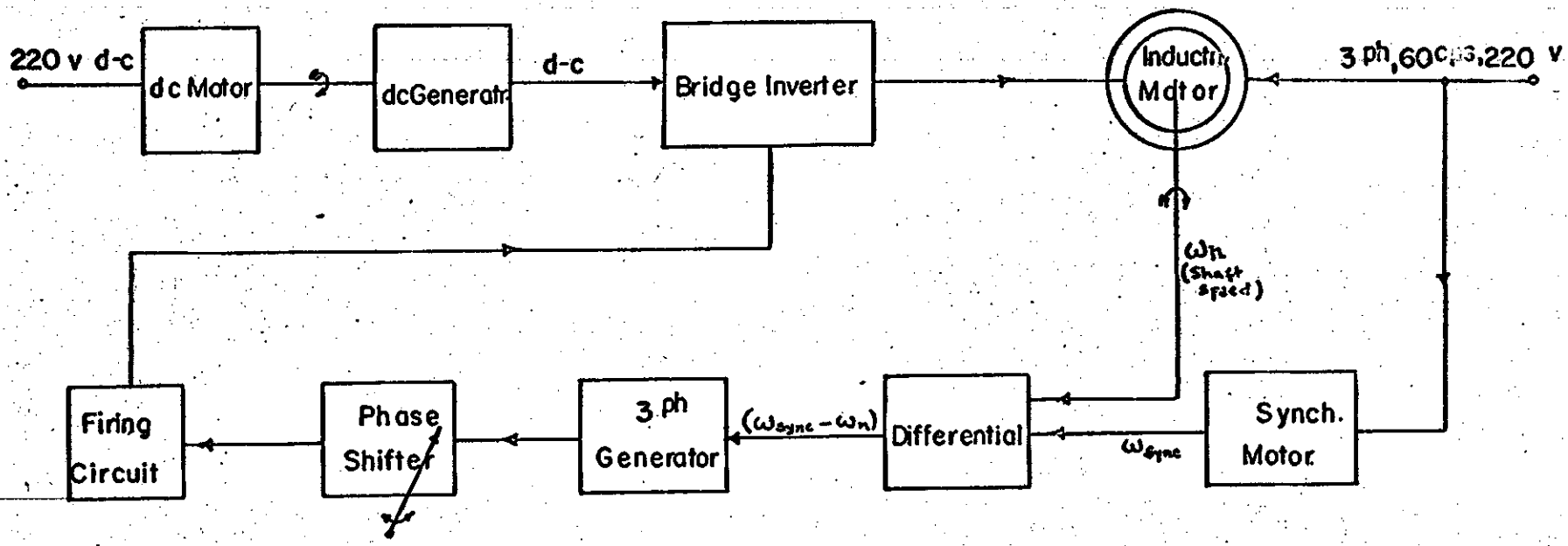

Figure 4-1 : Physical Test Set-Up.

this driving motor provided a means of calculating the torque of the induction motor at any speed.

The pertinent specifications for the various parts of the system are summarized hereunder.

Part	Specification
D.C. Generator	0 to 150 volts, reverse compounded separately excited. Short circuit current at 70V no load terminal voltage, 60 amperes.
Induction Motor	220 volts, 3 phase, 1200 rpm, 5 Hp wye connected stator, delta connected rotor, stator to rotor turns ratio per phase 2.0. Sum of the stator and rotor leakage reactances from lock rotor test, 1.904 ohms per phase of stator wye at 60 cps. Stator resistance 0.470 ohms per phase of stator wye, rotor resistance 0.334 ohms per phase of stator wye. The leakage reactance of the stator and rotor windings obtained from the manufacturers are 0.84 and 1.064 ohms per phase of stator wye respectively.

Part	Specification
Inverter	3 phase bridge connected using Westinghouse type 211E SCRs rated at 55 amps. r.m.s. current. Maximum gate signal to each element of the inverter, 100 ma at 10V.
Control Circuit	Designed to deliver six pulses of 6V and of 120 degrees duration (with respect to the voltage applied to the inverter), the leading edge of successive pulses being displaced in turn by 60 electrical degrees; alternate pulses isolated from ground and the other three pulses having a common ground connection.
Phase Shifter	Capable of symmetrically shifting the phases of the train of six pulses delivered from the control circuit with respect to the applied voltage to the inverter.

4.2 Summary of Test Procedure

4.2.1 Outline

Tests were performed in the laboratory using the test setup as shown in Fig. 4.1. The tests conducted can be classified into three major categories as follows:

(1) Tests on the inverter in the rotor circuit of the induction motor to study the conduction pattern and the behaviour of the inverter at various induction motor speeds.

(2) Torque measurements of the motor under standstill conditions.

(3) Torque measurements of the motor at different speeds with a view to establishing the general speed torque characteristics.

4.2.2 Tests to study the behaviour of the inverter

The various tests performed to study the conduction pattern and the behaviour of the inverter at various frequencies will now be described.

Fig. 4.2 indicates the equivalent circuit of the induction motor that was used for the evaluation of the conduction pattern under standstill conditions. This corresponds with the equivalent circuit developed in Section 3.1.1. The brush resistance and the external circuit resistance was found to be 0.125 ohms per phase at a value of rotor current equal to the r.m.s. value of the a.c. current at which the experiment was conducted. This is shown as R_e in Fig. 4.2.

The conduction equations evolved in Chapter 2 had to be modified to establish the conduction pattern in the induction motor. The conduction equations of Chapter 2, at each interval, consist of transient, steady state a.c. and

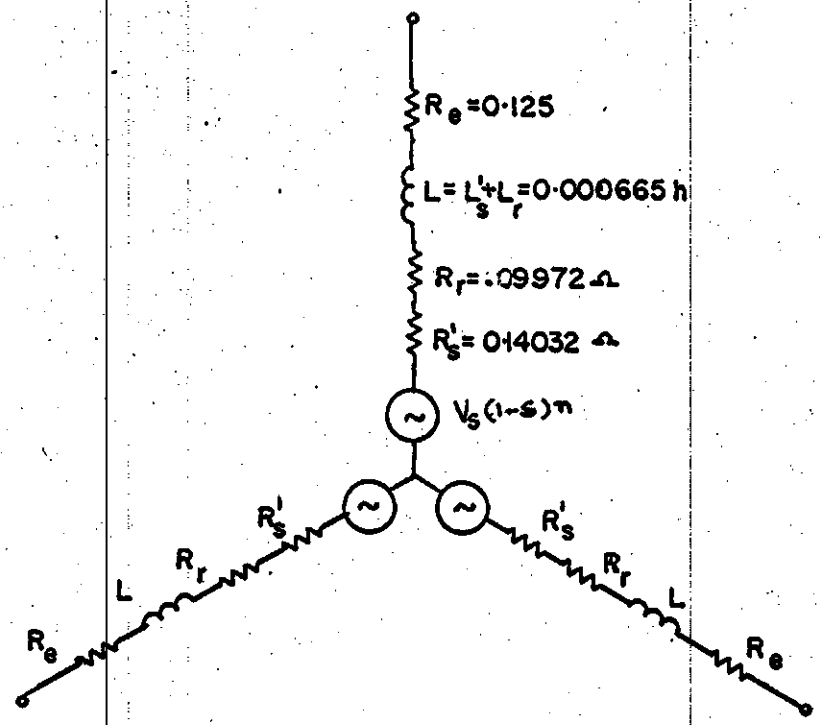

Figure 4·2: Equivalent Circuit of Experimental Motor.

d.c. component currents. The calculation of currents based on the sum of the rotor and the reflected resistance of the stator winding on the rotor, R'_s in Fig. 4.2, are valid only for a.c. quantities and time varying quantities. The reflected resistance of the stator winding was, therefore, not taken into account for calculating the d.c. currents in the conduction equations. It has been established[4] that the inductance observed from the rotor terminals is the sum of the leakage inductances of the stator and the rotor windings referred to the rotor windings. The transient and the a.c. component currents in the conduction equations, therefore, are controlled by the sum of the leakage inductances of the stator and the rotor phases shown by L in Fig. 4.2.

Using these relations in the program for the solution of conduction equations on the digital computer (Appendix 7.6), it was found that inversion under circuit conditions of Fig. 4.2 was impossible while the conduction pattern actually measured under experimental conditions was as shown by Curve 1 in Fig. 4.3.

In Section 2.2.3, it has been shown that the limit of inversion is decided by the firing delay (angle β_2) and the magnitude of current. In other words, for a given firing delay of the inverter, the inversion currents cannot be increased indefinitely (current can be increased by increasing the d.c. voltage or by reducing the circuit resistance) because the commutation of the currents should be complete

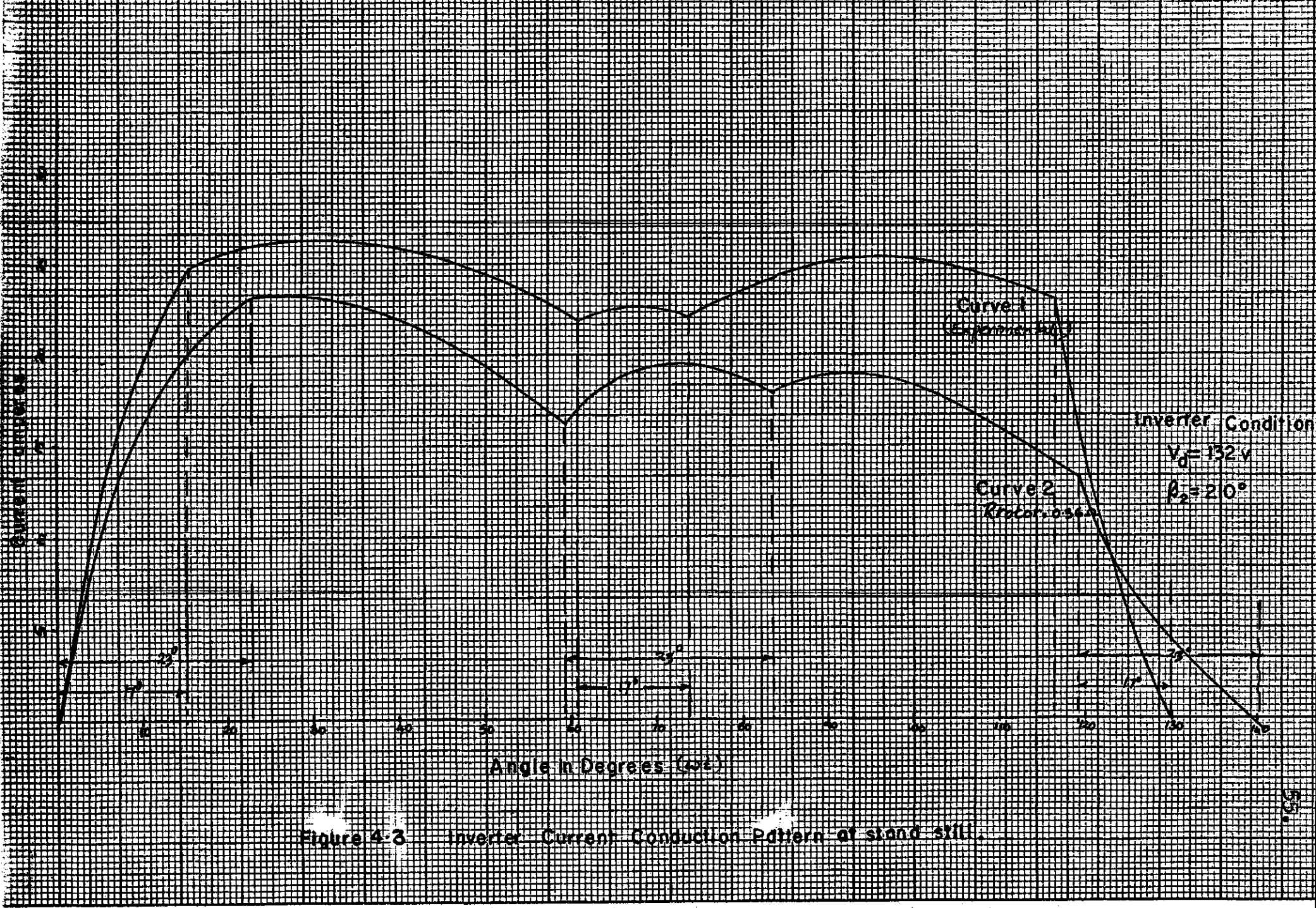

Figure 4-3 Inverter Current Conduction Pattern at stand still.

before the instants S, W, Z, etc. in Fig. 2.3. But, by assuming a resistance of 0.138 ohms in the rotor circuit, in addition to that of the resistances shown in Fig. 4.2, solution of the conduction equations yielded a current pattern as shown by Curve 2 of Fig. 4.3. This conduction pattern corresponds approximately to the observed conduction pattern on the oscilloscope during the experiment (Curve 1 of Fig. 4.3).

Similarly, an effective current of 11 amperes was measured in the rotor circuit for inversion parameters of: V_d = 63V, β_2 = 195 degrees, stator volts 220V line to line 3 phase and speed of the induction motor, 600 rpm corresponding to a slip of 0.5. The measured brush and the circuit resistance at this value of current was 0.12 ohms (value of R_e in Fig. 4.2). The solution of conduction equations indicated that inversion was impossible with these parameters.

Current patterns as shown by Curves 1 and 2 in Fig. 4.4 were obtained from the conduction equations by assuming an additional resistance of 0.340 ohms in the rotor circuit (total rotor circuit resistance of 0.463 ohms) and 0.32 ohms (total rotor circuit resistance of 0.6 ohms) respectively. The current pattern shown by Curve 2 of Fig. 4.4 corresponds roughly to the conduction pattern observed during the experiment.

The foregoing observations establish that the conduction patterns obtainable by solving the conduction equations

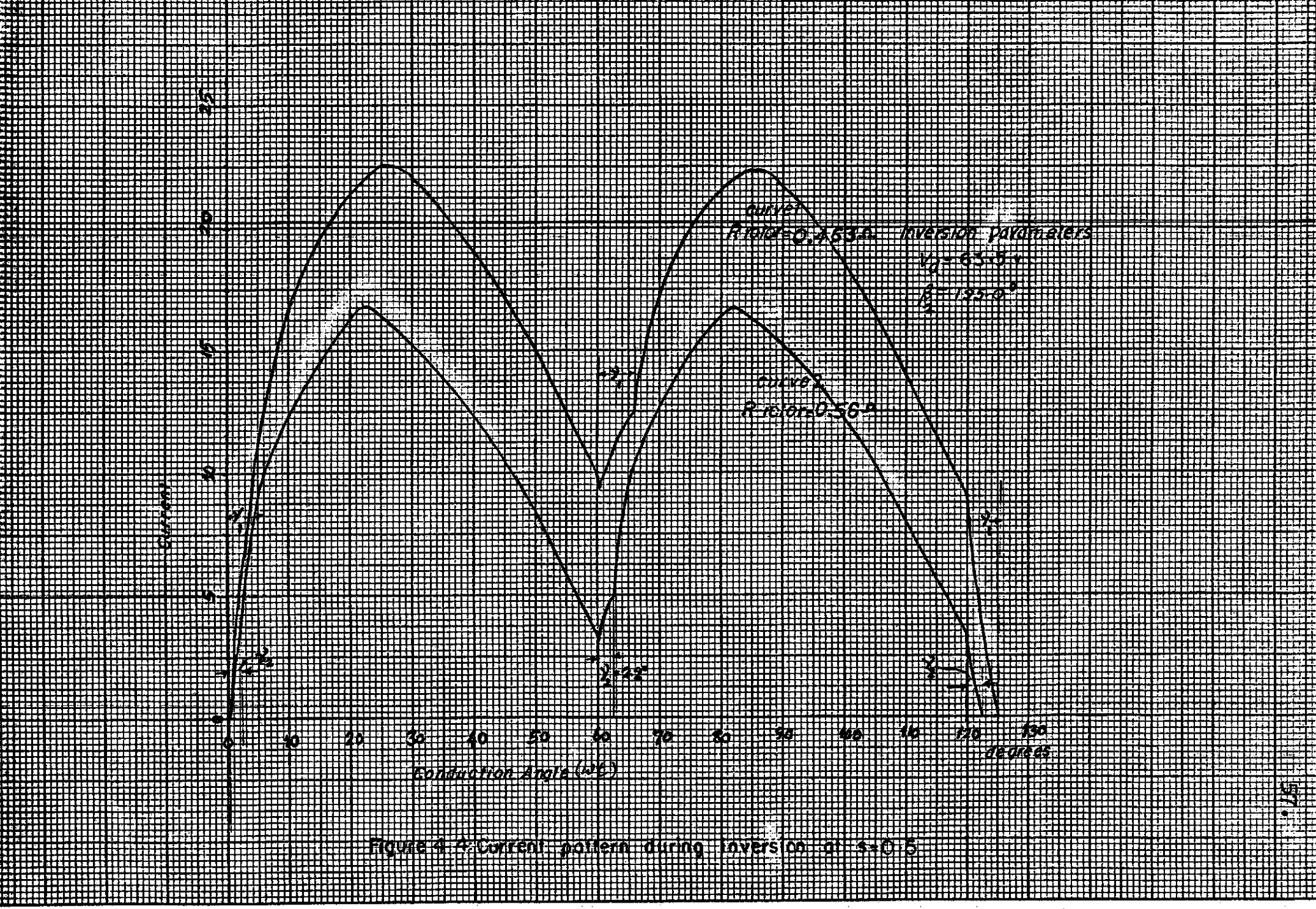

Figure 4.4 Current pattern during inversion at s=0.5

are dependent to a great extent on the circuit parameters. The conduction equations developed in Chapter 2 were under the assumption of zero impedance in the d.c. source. This assumption is, more or less, valid for a rectifier d.c. source. The generator used as the d.c. source for the experiments does not satisfy this assumption. Also, the small resistances of the rectifying elements which are complex functions of the currents have been neglected in the conduction equations. The brush resistance in the rotor of the induction motor is a function of the rotor current. The additional resistance assumed in the solution of the conduction equations to account for the effects made it possible to obtain correspondence between calculated and measured current patterns. The assumption that the inductance as seen from the rotor terminal is the sum of the leakage inductances of the rotor and the stator windings[4] is valid only if the stator resistance could be neglected. All these factors jointly contribute to the disparity between the calculated and the measured conduction patterns.

The conduction patterns obtained from the conduction equations by assuming an increased resistance in the rotor circuit (Curves 2 in Figs. 4.3 and 4.4 corresponding approximately to the measured patterns) were used for calculating the torque of the induction motor. Thus, the correctness of the torque equations derived in Chapter 3 could be checked.

4.2.3 Torque measurements of the motor under standstill conditions

The conduction patterns obtained above were used for torque calculations. The program written for the solution of the conduction equations (Appendix 7.3) also computed the Fourier coefficients of the conduction pattern. The Fourier coefficients served as the data for the calculation of the torque based on the equations derived under Section 3.3. It can be seen that the conduction patterns of Figs. 4.3 and 4.4 have no even harmonic components. The program based on these torque equations is discussed in detail in Appendix 7.6 Knowing the conduction pattern, therefore, the fundamental and the harmonic torques could be calculated.

Table 4.1 illustrates in a comparative manner the performance of the induction motor under running conditions, specifically,

(1) as a conventional short circuited rotor induction motor

(2) as an inverter fed rotor motor.

Both calculated and measured results for (2) are given.

Table 4.1 Comparison of Torque Values

Torque in Foot Lbs.		Slip	Rotor Current (Amperes)	Running Conditions
Measured	Calculated			
22.0 braking	34.0 braking	1	21	Inverter fed rotor motor at standstill
11.75 braking	10.58 braking	0.5	11.5	Inverter fed rotor motor at 600 rpm.
	21.0 motoring	1	120	Conventional short circuited rotor motor at standstill
	60.0 motoring	0.2	40	Conventional short circuited rotor motor running at 960 rpm.

A sample print-out of the torque values on the digital computer for the two conditions investigated above can be found in Appendix 7.6.

The disparities between the observed and the calculated torque values can be attributed to various reasons such as magnetic circuit dissymmetry, variation of harmonic impedance of the rotor, etc. The main reason for the disparity in the above-mentioned calculations is that the conduction pattern on which the torque calculations were based was only arbitrarily chosen to correspond approximately to the actual conduction pattern. The abovesaid observations establish that the torque of the induction motor under conditions of inversion in the rotor can be determined to a fair degree of

accuracy if the conduction pattern in the rotor is known.

4.2.4 Speed torque characteristics

The rotor voltage of the induction motor decreases as the speed increases in the forward direction. For a constant d.c. voltage applied to the inverter, therefore, the magnitude of the inversion currents in the rotor increased with the forward speed of the induction motor. (The forward direction of rotation of the motor is defined as that along the direction of rotation of the magnetic field.) The braking torque was, consequently, found to increase with the speed of the induction motor, other parameters of the inverter being constant. Due to the same reasons, the braking torque of the motor was found to increase with the d.c. voltage applied to the inverter when the speed of the motor was constant.

Further, it was observed during the experiment that the torque of the motor increased with the firing delay angle. After a maximum value of the firing delay angle (β_2 in the conduction equations) the torque was found to decrease for any further increase in the delay angle. It is felt that this effect was due to the phase relations of the rotor and the stator mmfs. This effect was not investigated in detail.

The torque at various speeds could not be measured due to limitations of the test setup. The main limitation of the test setup was the lack of protection against high fault currents that may result from commutation failure. The motor

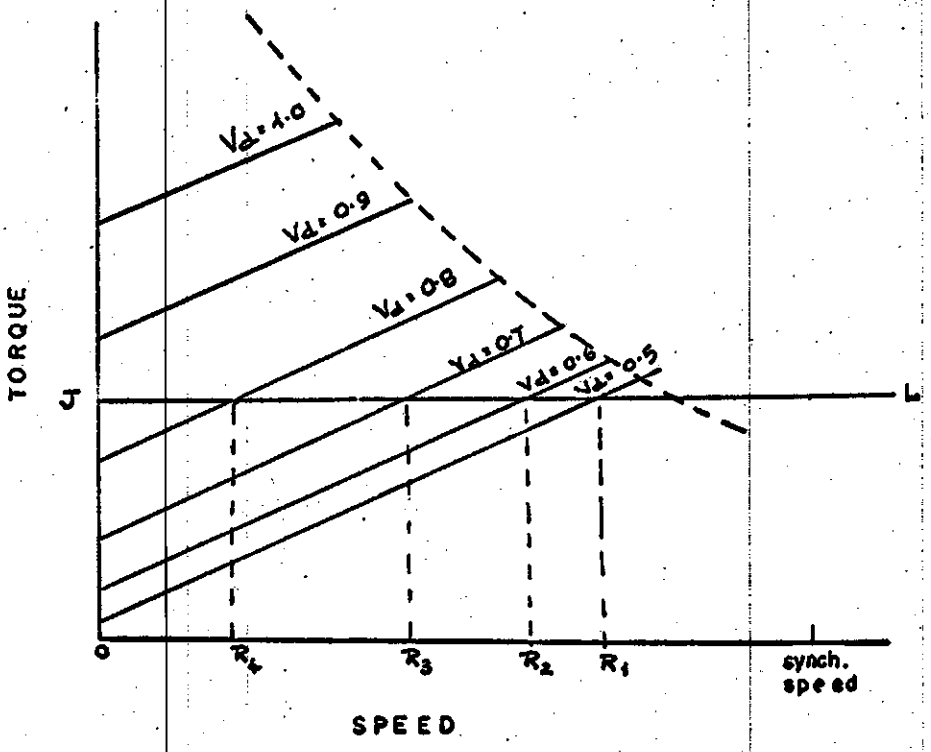

FIGURE 4.5: TORQUE SPEED RELATIONS

torque was, however, measured at slow speeds and low d.c. voltages to predict the general form of the torque speed characteristics.

The general form of the characteristics that could be predicted from these limited measurements is shown in Fig. 4.5. The dotted lines in the figure indicate the limiting speed of the motor for successful inversion. Beyond this speed given by the dotted line, the inversion currents will grow in magnitude; therefore, the commutation of current cannot be completed before the limiting instants such as S, W, Z, etc. shown in Fig. 2.3. For a constant d.c. voltage applied to the inverter and a constant firing delay angle, there is a limiting speed of the motor beyond which inversion cannot possibly take place.

The torques shown in Fig. 4.5 are braking torques. If the motor has an overhauling load* which may be represented by the line JL in Fig. 4.4, the motor will have stable running speeds anywhere between R_1, R_2, R_3 depending on the parameters of inversion.

It was observed during the experiment that the energy returned to the supply mains across the air gap and the stator winding was in excess of the d.c. energy input into the inverter. The additional energy was derived from the d.c. motor driving the induction motor.

---

* Cranes and hoists, while lowering their loads and locomotives during retardation, are examples of overhauling load operations.

A continuous control of the inversion parameters (d.c. voltage and delay angle) of this drive scheme will, therefore, result in the operation of the induction motor as a regenerative brake at any desired speed between standstill and the normal running speed. Regenerative braking is possible in the normal operation of the induction motor only at speeds above the synchronous speed.

5. CONCLUSIONS AND RECOMMENDATIONS

5.1 Conclusions

5.1.1 Conduction equations

The method adopted for the evolution of the conduction pattern is free from the assumptions made regarding the current wave shape in the literature.[5-9] The conduction equations and the equivalent circuit developed offer a better insight into the mechanism of inversion.

5.1.2 Torque equations

The torque equations derived in Chapter 3 and the analysis of the torque based on the generalized machine theory offer an elegant method for the general analysis of motor torques under harmonic current conditions.

The torque values obtained indicate that the torque equations can be successfully employed for the torque calculations of such a drive, if the correct conduction pattern can be obtained. The approximations regarding the equivalent circuit representation of the induction motor (Ch.3) should not adversely affect the accuracy of the torque calculations.

5.1.3 Drive characteristics

In spite of the limitations of the experimental setup, the general shape of the torque speed characteristics could be established. The characteristics appear to fit in very well with the requirements of hoist or traction drives as a dynamic brake.

5.2 Recommendations for Further Work

(1) Theoretical analysis of the conduction equations taking the effects of the d.c. source impedance and the non-linear resistances due to such things as the diode and brush resistance to establish a correct conduction pattern can be undertaken to establish the equivalent circuit of the inverter accurately.

(2) The slope of the torque speed curves in Fig. 4.5 can be changed by varying the d.c. voltage applied to the inverter. Investigations regarding a closed loop d.c. voltage control for the inverter may be carried out with a view to obtaining the desired characteristics.

(3) An experimental setup to hoist and lower loads may be set up with an improved firing circuit for the inverter consisting of a sophisticated protection device. Such a set-up would facilitate the studies on the characteristics and the transient behaviour of the drive.

(4) From the foregoing investigations, design parameters for such a drive scheme could be optimized.

5.3 Concluding Remarks

The purpose of this investigation was to establish the general characteristics of a drive employing a wound rotor induction motor with an inverter in the rotor circuit. The torque-speed characteristics of the drive were found to compare favourably with those of the conventional d.c. systems.

The relative merits of this drive scheme over the conventionally adopted d.c. drive schemes can be evaluated precisely only after further detailed investigations are carried out as outlined in Section 5.2.

6. REFERENCES

1. Lamb, C.St.J., 1963, "Commutatorless Alternating-voltage-fed Variable-speed Motor", Proceedings of the Institution of Electrical Engineers, Vol. 110, No. 12, December, pp.2221-2227.

2. Bradley, D.A., Clarke, C.D., Davis, R.M., Jones, D.A., 1964, "Adjustable-Frequency Inverters and their Applications to Variable-speed Drives", Proceedings of the Institution of Electrical Engineers, Vol. 111, No. 12, November, pp.1833-1846.

3. Erlicki, M.S., Ben Uri, J., Wallach, Y., 1963, "Switching Drive of Induction Motors", Proceedings of the Institution of Electrical Engineers, Vol. 110, No. 8, August, pp.1441-1450.

4. Bland, R.J., Hancock, N.N., Whitehead, R.W., 1963, "Considerations Concerning a Modified Kramer System", Proceedings of the Institution of Electrical Engineers, Vol. 110, No. 12, December, pp.2228-2232.

5. Ressik, H., 1941, Mercury Arc Current Converters, Issac Pitman and Co., London, England.

6. Read, J.C., 1945, "The Calculation of Rectifier and Inverter Performance Characteristics", Journal of the Institution of Electrical Engineers, Vol92,II, pp.495-509

7. Knight, H.deB., 1960, The Arc Discharges and its Applications to Power Control, Chapman and Hall, London, England.

8. Ludbrook, A., Murray, R.M., 1965, IEEE International Convention Record, part 8, pp.121,127.

9. Adamson, C., Hingorani, N.G., 1960, High Voltage Direct Current Power Transmission, Garravoy Ltd., London, England.

10. Wallach, Y., Erlicki, M.S., Ben Uri, J., 1963, "Multi-phase Rectifier Currents", Proceedings of the Institution of Electrical Engineers, Vol. 110, No. 8, August, pp.1434-1440.

11. Fitzgerald, A.E., Charles Kingsley, Jr., 1961, Electrical Machinery, McGraw-Hill Book Company, Inc., New York.

12. Puchstein, A.F., Lloyd, T.C., Conrad, A.G., 1958, Alternating-Current Machines, John Wiley and Sons, Inc., New York.

13. Bernard Adkins, 1959, The General Theory of Electrical Machines, John Wiley and Sons, Inc., New York.

14. Kron Gabriel, 1959, Tensors for Circuits, Dover Publications Inc., New York 14.

15. Yao-Nan Yu, 1963, "The Torque Tensor of the Generalized Machine", Power Apparatus and Systems, Transaction papers of the A.I.E.E., February, pp.623-629.

7. APPENDICES

7.1 Note on the Design of the Firing Control Circuit

7.1.1 Requirements of firing circuit

The bridge connected inverter must be supplied with firing power to each of the gates of the six elements at the appropriate instant. All the six elements should be fired sequentially at 60 electrical degrees and the instant of the firing should be capable of being shifted in phase with respect to the main three phase a.c. supply connected to the inverter.

The firing power to each of the gates can be in the form of steep pulses but, it has been shown in Section 2.2.2 that the pulses must last at least sixty electrical degrees to make the rectifier/inverter self starting. The pulses cannot be more than 120 degrees in duration because the period of conduction through each element is 120 degrees plus the time for the decay of the current, i.e. the commutation angle. The elements 1, 3 and 5 have a common terminal (Fig. 2.2) and can be supplied with firing power with respect to the common terminal. The elements 4, 2 and 6, however, do not have a common connection and, therefore, the firing power to these elements must be isolated from one another.

7.1.2 Operation of the firing circuit

Fig. 7.2 is a circuit diagram of the control circuit. The terminals A, B and C are connected to a three

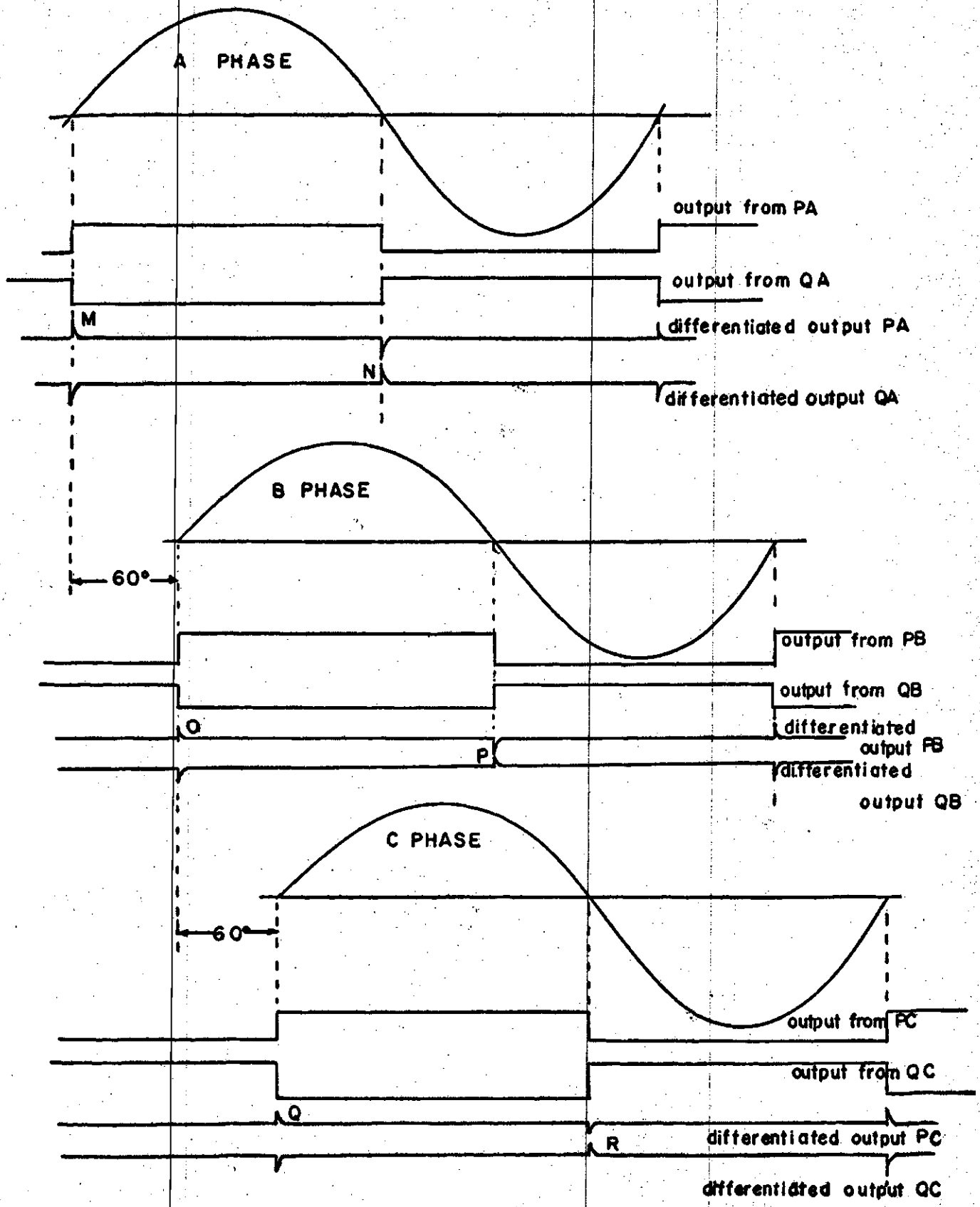

Figure 7·1 : Wave Shapes and Pulse Relations

phase a.c. supply at the same frequency as that of the inverter supply. The resistors R_{1A}, R_{1B} and R_{1C} in the figure create a neutral point at the earth terminal from the three phase supply. The control circuit is exactly similar for each phase and the working of one phase is similar to that of the others. The working of phase A is as follows. The transistor T_{1A} conducts when the a.c. voltage is positive and, therefore, transistor T_{3A} is supplied with positive voltage when the a.c. voltage is negative. The output at point P_A will, therefore, be a positive pulse of 180 degrees duration (referred to the 3 phase a.c. supply). The transistor T_{2A} being a p-n-p device, conducts when the voltage of the a.c. wave is negative. The output from point Q_A is a negative pulse of 180 degrees duration, being negative when the a.c. voltage is positive. The output from the terminals P_A, P_B, P_C, Q_A, Q_B and Q_C in relation to the a.c. wave is shown in Fig. 7.1.

The condensers C_{2A} and C_{1A} (Fig. 7.2) differentiate the pulses from the terminals P_A and Q_A, and the diodes eliminate the negative spikes. The outputs at terminals A-, A+, B-, B+, C- and C+ will only be the positive spikes. Referring to Fig. 7.1, the positive spikes M, N, O, P, Q and R appear at the A+, A-, B+, B-, C+ and C- terminals respectively in Fig. 7.2. The transistors T_{4A}, T_{5A} and T_{6A}, T_{7A} form two identical bistable flip flop circuits. The bases of the two transistors are connected to the triggering pulses from the

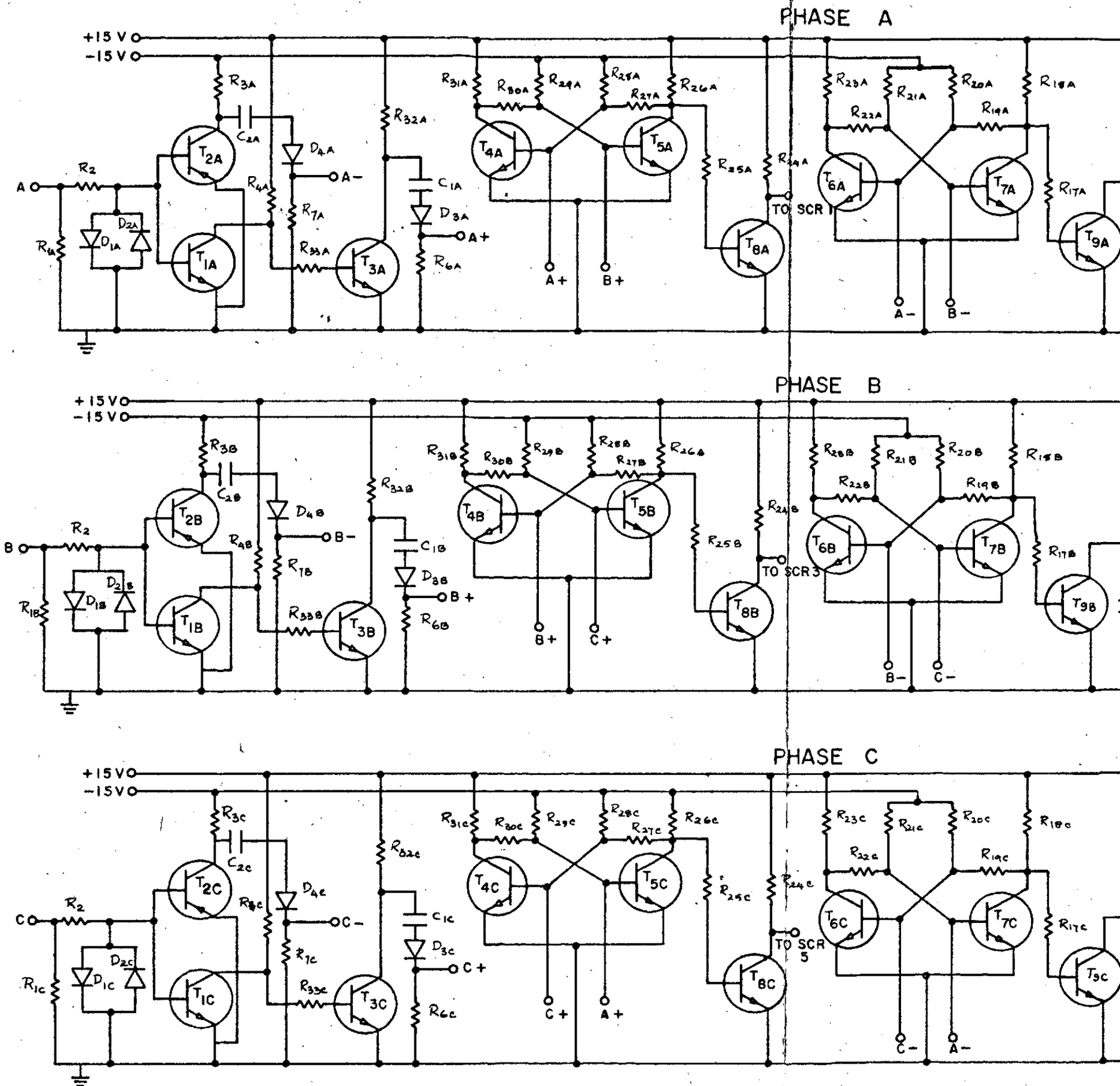

Figure 7.2: The Firing Circuit.

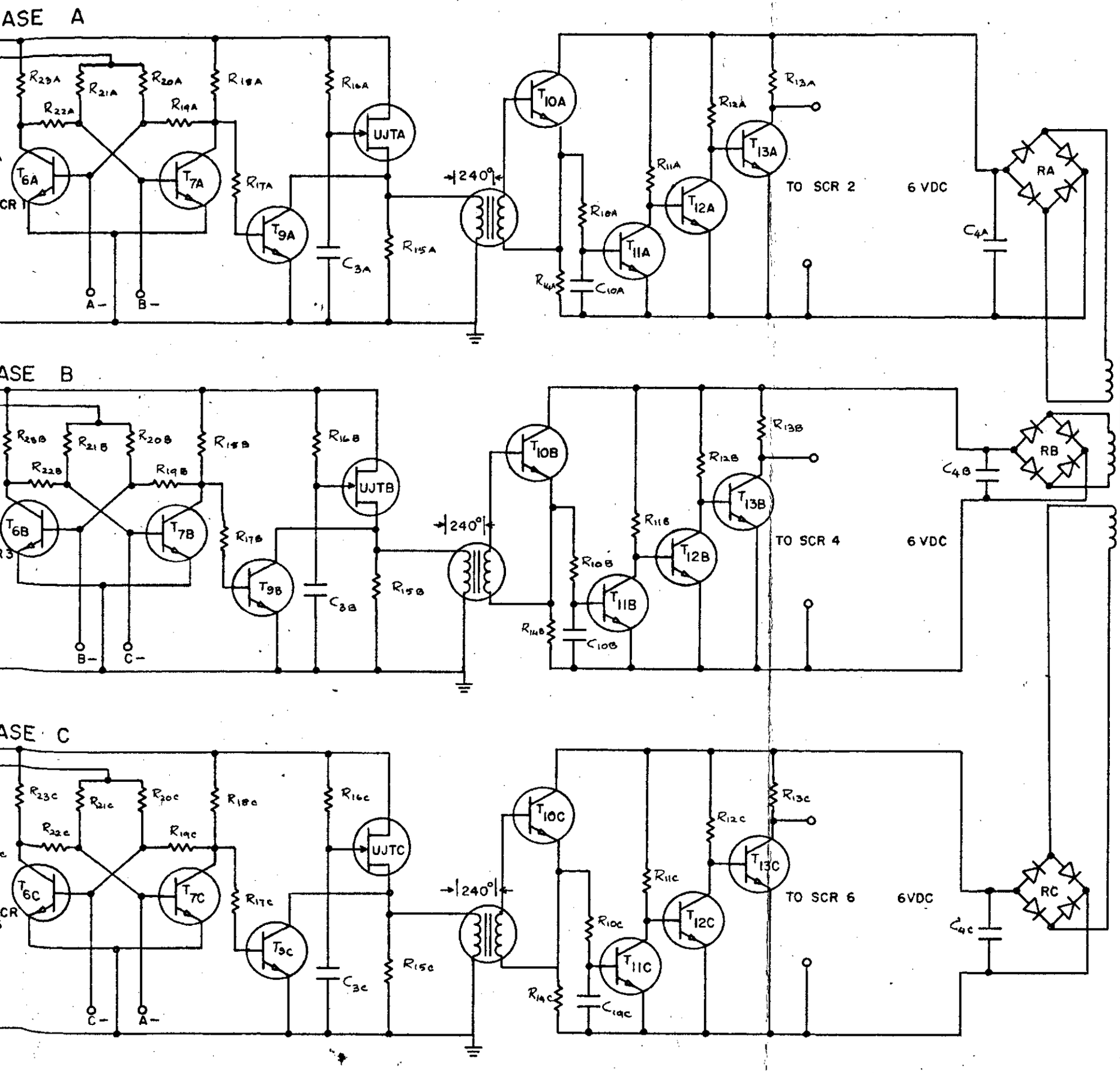

7.2: The Firing Circuit.

COMPONENT VALUES

$T_1, T_3, T_4, T_5, T_6, T_7, T_8, T_9, T_{11}, T_{12}, T_{13}$	2N1306
T_2	2N1307
T_{10}	2N2160
$R_1, R_6, R_4, R_3, R_{32}, R_{25}, R_{12}$	1K
$R_{33}, R_{31}, R_{26}, R_{23}, R_{18}, R_{11}$	1.2K
$R_{30}, R_{27}, R_{22}, R_{19}, R_{17}$	15K
$R_{29}, R_{28}, R_{21}, R_{20}$	52K
R_{11}	2.2K
R_{13}	27
R_2	270
R_{16}	3.3K
R_{15}	100
R_{14}	10
R_{10}	330
R_7	10K
C_2, C_1	3000pf 450V
C_3	33000pf 450V
C_{10}	1 uf, 10V
C_4	100 uf, 15V
D_1, D_2	IN625

terminals A-, A+, B-, B+, C- and C+. The flip flop formed by T_{4A} and T_{5A} is connected to terminals A+ and B+ which trigger the transistors by two pulses 120 degrees apart (pulses M and O in Fig. 7.1) and the transistors T_{6A} and T_{7A} are connected to terminals A- and B- which trigger the transistors by two pulses 120 degrees apart (pulses N and P in Fig. 7.1). The transistors T_{4A} and T_{6A}, therefore, conduct for 120 electrical degrees and the output from the collector terminals of T_{5A}— a 120 degrees wide positive pulse—is amplified by T_{8A} and supplied to the gate terminal of SCR1. Similarly, the output pulses from the other two phases are also supplied to the SCRs 3 and 5. These pulses are positive with respect to ground and can be supplied to the gates of the SCRs 1, 3 and 5 having a common connection. The output pulses from T_{8A}, T_{8B} and T_{8C} are displaced in time by 120 electrical degrees.

It has been pointed out that the elements of 4, 2 and 6 must have their gate power isolated from the ground terminal. A unijunction transistor relaxation oscillator, one for each phase, generates saw tooth pulses. The output saw tooth wave from the UJTA is grounded for 120 degrees of supply frequency through the transistor T_{9A}, switched by the output of the bistable flip flop circuit consisting of transistors T_{6A} and T_{7A}. The pulse output for 240 degrees of the supply frequency is amplified by a high beta silicon transistor T_{10A}. The transistor T_{11A} serves as a power amplifier to the input pulses which are isolated from the UJT circuit (and

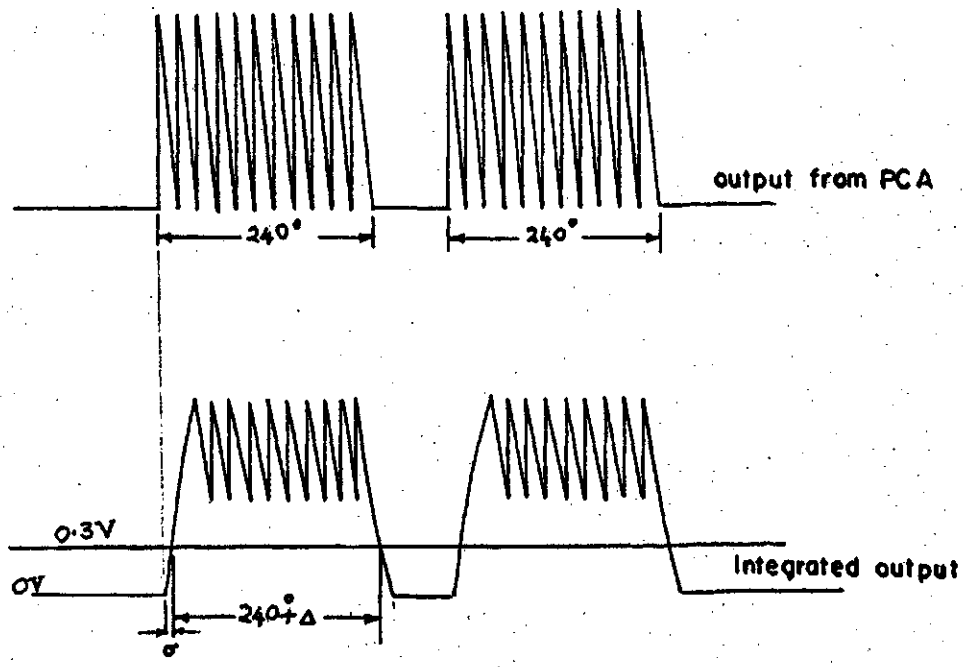

FIGURE 7·3: CONTROL CIRCUIT WAVEFORMS

hence from ground) by a small ferrite core pulse transformer PCA. The amplified output from the transistor T_{10A} is integrated by resistor R_{10A} and capacitor C_{10A}. The input wave form to the integrating circuit and the output from the integrating circuit is shown in Fig. 7.3. The output of the integrating circuit switches transistor T_{11A} for about 240 degrees and the output from the collector terminal is a 120 degrees wide pulse. To improve the pulse wave shape, the output pulse from T_{11A} is made the base signal to the switch formed by transistor T_{12A}. The collector output from transistor T_{12A} is a pulse 240 degrees wide isolated from ground. A pulse of 120 degrees wide may be employed at the pulse transformer PCA to result in a 120 degrees pulse at the output of transistor T_{12A}; but, the pulse distortion at the integrating circuit would make the output from T_{12A} wider than 120 degrees. It has been established that the maximum width of the pulse to the gates of the SCRs can be 120 degrees in a 3 phase bridge connection and the minimum pulse width for a self-starting rectifier-inverter is 60 degrees. Therefore, by starting with a 240 degrees wide pulse at the pulsing transformers PC, the output from the transistor T_{12A} is slightly wider than 240 degrees. This pulse is utilized as the control for the switching transistor T_{13A}, the output from which will be a pulse slightly less than 120 degrees by a small amount Δ and the output from T_{13A} will be delayed by a small angle σ. The angle σ will be too small to considerably affect the

working of the SCR's. The angles Δ and σ are shown in Fig. 7.3.

The d.c. supply for generating these three pulses isolated from ground is derived from three small bridge rectifier sources—RA, RB and RC. The three d.c. output voltages are isolated from ground and from one another. The three output pulses from transistors T_{13A}, T_{13B} and T_{13C} are employed to fire the SCR elements 4, 6 and 2 of the inverter.

The phase position of the firing pulse train with respect to the a.c. voltage wave form applied to the inverter can be varied by changing the phase of the control a.c. signal to terminals A, B and C (Fig. 7.1). This is achieved by rotating the stator of the small 3 phase a.c. generator which forms the control voltage source to the firing control circuit. The drive for this control signal generator has been discussed in detail in Chapter 4.

7.2 Solution of the Conduction Differential Equations

All the differential equations are linear and are of first order.

Interval 1

$$3I_{2(1)}(pL + R) = 2V_B - (V_R + V_d + V_Y) \qquad (7.1)$$

Substituting

$$V_R = V_m \sin (\omega t + \frac{\pi}{6} + \beta_2) \qquad (7.2)$$

$$V_Y = V_m \sin (\omega t - \frac{2\pi}{3} + \frac{\pi}{6} + \beta_2) \qquad (7.3)$$

$$V_B = V_m \sin\left(\omega t + \frac{2\pi}{3} + \frac{\pi}{6} + \beta_2\right) \qquad (7.4)$$

and simplifying,

$$3I_{2(1)}(pL + R) = +\frac{V_m K_1}{2} \sin \omega t - \frac{V_m K_2}{2} \cos \omega t - V_d \qquad (7.5)$$

where

$$K_1 = (-3\sqrt{3} \cos \beta_2 - 3\sin \beta_2)/6 \qquad (7.6)$$

$$K_2 = (3\sqrt{3} \sin \beta_2 - 3 \cos \beta_2)/6 \qquad (7.7)$$

The particular integral is

$$\frac{K_1 V_m}{Z} \sin(\omega t - \phi) - \frac{K_2 V_m}{Z} \cos(\omega t - \phi) - \frac{Vd}{3R} \qquad (7.8)$$

where

$$Z = \sqrt{R^2 + X^2}$$

and

$$\phi = \tan^{-1} X/R$$

The complementary function is

$$C_1 \epsilon^{-Rt/L} \qquad (7.9)$$

The complete solution is

$$C_1 \epsilon^{-Rt/L} + \frac{K_1 V_m}{Z} \sin(\omega t - \phi) - \frac{K_2 V_m}{Z} \cos(\omega t - \phi) - \frac{Vd}{3R} \qquad (7.10)$$

<u>Interval 2</u>

$$2I_{2(2)}(pL + R) = V_B - V_R - V_d \qquad (7.11)$$

Substituting

$$V_R = V_m \text{ Sin } (\omega t + \frac{\pi}{6} + \beta_2 + \gamma) \qquad (7.12)$$

$$V_Y = V_m \text{ Sin } (\omega t + \frac{\pi}{6} - \frac{2\pi}{3} + \beta_2 + \gamma) \qquad (7.13)$$

$$V_B = V_m \text{ Sin } (\omega t + \frac{\pi}{6} + \frac{2\pi}{3} + \beta_2 + \gamma) \qquad (7.14)$$

The complementary function is

$$C_2 \epsilon^{-Rt/L} \qquad (7.15)$$

and the particular integral is

$$- \frac{K_3 V_m}{Z} \text{ Sin } (\omega t - \phi) - \frac{K_4 V_m}{Z} \text{ Cos } (\omega t - \phi) - \frac{Vd}{2R} \qquad (7.16)$$

where

$$K_3 = \frac{\sqrt{3}}{2} \text{ Cos } (\beta_2 + \gamma) \qquad (7.17)$$

$$K_4 = \frac{\sqrt{3}}{2} \text{ Sin } (\beta_2 + \gamma) \qquad (7.18)$$

Interval 3

$$3I_{2(3)}(pL + R) = 2V_B - V_R - V_Y - 2V_d \qquad (7.19)$$

substituting

$$V_R = V_m \text{ Sin } (\omega t + \frac{\pi}{2} + \beta_2) \qquad (7.20)$$

$$V_Y = V_m \text{ Sin } (\omega t - \frac{\pi}{6} + \beta_2) \qquad (7.21)$$

$$V_B = V_m \text{ Sin } (\omega t - \frac{5\pi}{6} + \beta_2) \qquad (7.22)$$

The complementary function is

$$C_3 \epsilon^{-Rt/L} \tag{7.23}$$

and the particular integral is

$$-\frac{K_5 V_m}{Z} \text{Sin } (\omega t-\phi) - \frac{K_6 V_m}{Z} \text{Cos } (\omega t-\phi) - \frac{2Vd}{3R} \tag{7.24}$$

where

$$K_5 = (-3\sqrt{3} \text{ Cos } \beta_2 - 3 \text{ Sin } \beta_2)/6 \tag{7.25}$$

$$K_6 = (3 \text{ Cos } \beta_2 + 3\sqrt{3} \text{ Sin } \beta_2)/6 \tag{7.26}$$

Interval 4

The equation is,

$$2I_{2(4)}(pL + R) = V_B - V_Y - V_d \tag{7.27}$$

substituting

$$V_R = V_m \text{ Sin } (\omega t + \frac{\pi}{2} + \beta_2 + \gamma) \tag{7.28}$$

$$V_Y = V_m \text{ Sin } (\omega t - \frac{\pi}{6} + \beta_2 + \gamma) \tag{7.29}$$

$$V_B = V_m \text{ Sin } (\omega t - \frac{5\pi}{6} + \beta_2 + \gamma) \tag{7.30}$$

The complementary function will be

$$C_6 \epsilon^{-Rt/L} \tag{7.31}$$

and the particular integral is

$$-\frac{K_7 V_m}{Z} \text{Sin } (\omega t-\phi) - \frac{K_8 V_m}{Z} \text{Cos } (\omega t-\phi) - \frac{V_d}{2R} \tag{7.32}$$

where

$$K_7 = \frac{\sqrt{3}}{2} \text{Cos } (\beta_2 + \gamma) \qquad (7.33)$$

$$K_8 = \frac{\sqrt{3}}{2} \text{Sin } (\beta_2 + \gamma) \qquad (7.34)$$

Interval 5

The equation is,

$$3I_2 (pL + R) = 2V_B - (V_R + V_d + V_Y) \qquad (7.35)$$

substituting

$$V_R = V_m \text{ Sin } (\omega t + \frac{5\pi}{6} + \beta_2) \qquad (7.36)$$

$$V_Y = V_m \text{ Sin } (\omega t + \frac{\pi}{6} + \beta_2) \qquad (7.37)$$

$$V_B = V_m \text{ Sin } (\omega t + \frac{\pi}{2} + \beta_2) \qquad (7.38)$$

The complementary function is

$$C_5 \epsilon^{-Rt/L} \qquad (7.39)$$

and the particular integral will be

$$\frac{V_m}{Z}[K_9 \text{ Sin } (\omega t - \phi) - K_{10} \text{ Cos } (\omega t - \phi)] - \frac{Vd}{3R} \qquad (7.40)$$

where

$$K_9 = \text{Sin } \beta_2 \qquad (7.41)$$

$$K_{10} = \text{Cos } \beta_2 \qquad (7.42)$$

7.3 Digital Computer Program For the Solution of Conduction Equations

The conduction equations derived in Chapter 2 are solved by an iterative process on a digital computer. A small value of γ, the commutation angle, is assumed initially and the equations are solved to find the current at the end of interval 5. If the correct value of γ has been assumed, the current at the end of interval 5 will be zero. If the current is not zero at the end of interval 5, the value of γ is successively incremented by small values and the calculations are repeated until the current at the end of interval 5 is zero.

Fig. 7.4 indicates the program logic in a block diagram. In addition, the program written in Fortran IV is also listed. The input data to the program must be given in the following order: stator resistance per phase, stator inductance in henries per phase, rotor resistance per phase of wye, rotor inductance per phase of wye, firing angle β_2, d.c. voltage applied to the inverter, a.c. phase voltage (rms value) applied to the stator, angular velocity (radians per sec.) of rotor voltages, turns ratio of the stator turns per phase to the rotor turns per phase of wye, slip of the induction motor and W, a program control number. The format for these values in the data card is,

F8.4, F8.5, F8.4, F8.5, F6.1, 2F7.2, F8.3, F7.4, and 2F4.1.

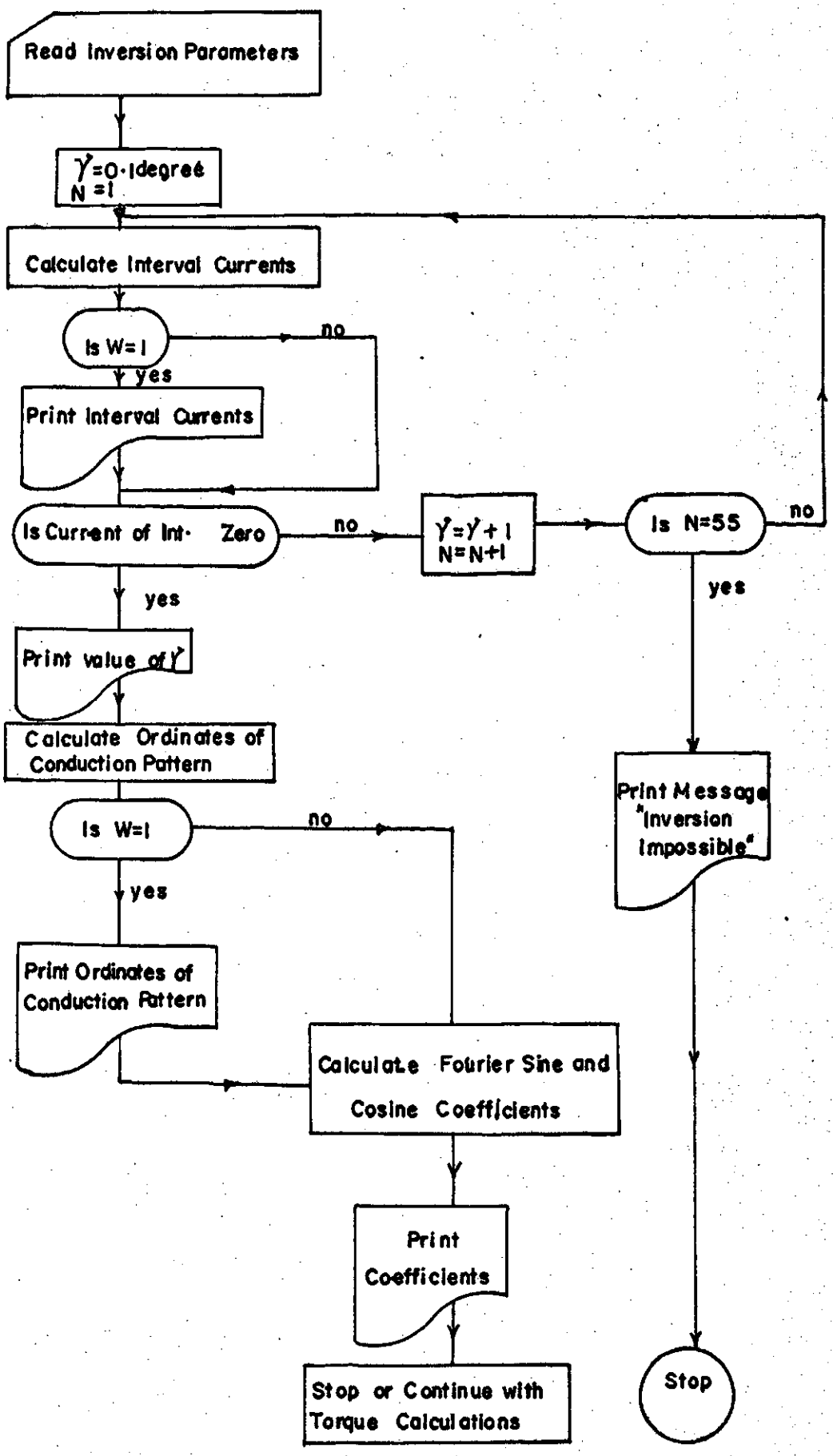

Figure 7·4: Block Diagram of Logic for the Solution of Conduction Equations·

Table 7.1, Card listings of the Program for the Solution of Conduction Equations

```
  301 READ(5,20)OHM1,HEN1,OHM2,HEN2,DELAY,QNVD,ACVO,OMEGAS,TURN,S,W,GAMA
  949 DCVO3-NVDM
   20 FORMAT(F8.4,F8.5,F8.4,F8.5,F6.1,F7.2,F7.2,F8.3,F7.4,F4.1,F4.1,F5.1
     1)
      OMEGA=OMEGAS*S
      FICT=(HEN1+HEN2)*OMEGA
      N=1
      HENRY=HEN1+HEN2
     OCOMPLEXARTF,ACA,ACB,ACC,ACD,ACE,ACQR1,ACQR2,AB,BB,CMVEA,CMVEB,STM1
     1,STM2,STDRES,STDD,STDC,STDA,STDB,STDR1,STDR2,VECT1,VECT3,VECT5,VEC
     2T7,VECT9,VECT11,ACNETC,TQCLN
      RESIST=OHM1+OHM2
      POW=-RESIST/HENRY
      ARTF=CMPLX(RESIST,FICT)
      PHI=ATAN2(FICT,RESIST)
      Z=CABS(ARTF)
      SQ=SQRT(3.0)
      VSPED=ACVO*TURN*OMEGA*SQRT(2.0)/OMEGAS
      OHM=OHM2
      WRITE(6,956)Z,OHM
      B=VSPED/Z
      WRITE(6,956)B,RESIST
      ALPHA=DELAY*3.1428/180.0
      WRITE(6,956)ALPHA,FICT
  956 FORMAT(1H1,2F10.5)
      IF(W-1.0)11,947,947
  947 WRITE(6,950)
  950 FORMAT(1H1,39H CONVERGENCE TEST FOR COMMUTATION ANGLE)
      WRITE(6,990)
  990 FORMAT(1H ,61HINTERVAL1  INTERVAL2  INTERVAL3  INTERVAL4  INTERVAL
     15    GAMA)
   11 GAMA=0.2
   10 RADS1=(GAMA/180.0)*3.1428
      TIME1=RADS1/OMEGA
      ABC=(-3.0*SQ*COS(ALPHA)-3.0*SIN(ALPHA))/6.0
      BCD=(SQ*3.0*SIN(ALPHA)-3.0*COS(ALPHA))/6.0
      CDE=COS(ALPHA+RADS1)*SQ/2.0
      DEF=ABC
      XYZ=SQ*SIN(ALPHA+RADS1)/2.0
      ANGLE=(60.0/180.0)*3.1428-RADS1
      PERIO=ANGLE/OMEGA
      WRITE(6,957)PERIO,RADS1
  957 FORMAT(2F10.6)
      EFG=(3.0*COS(ALPHA)+3.0*SQ*SIN(ALPHA))/6.0
      GHI=SQ*COS(ALPHA+RADS1)/2.0
      HAB=SQ*SIN(ALPHA+RADS1)/2.0
      CONA=B*(ABC*SIN(PHI)+BCD*COS(PHI))+DCVO/(3.0*OHM)
      PORT1=B*(ABC* SIN(RADS1-PHI)-BCD* COS(RADS1-PHI))
      AMP1=CONA*(2.7183**(POW*TIME1))+PORT1-DCVO/(3.0*OHM)
      CONB=AMP1-B*(CDE* SIN(PHI)-XYZ* COS(PHI))+DCVO/(2.0*OHM)
      PICE2=B*(CDE* SIN(ANGLE-PHI)+XYZ* COS(ANGLE-PHI))
      AMP2=CONB* (EXP(POW*PERIO))-PICE2-DCVO/(2.0*OHM)
      CONC=AMP2+B*(DEF* SIN(PHI)+EFG* COS(PHI))+2.0*DCVO/(3.0*OHM)
      BIT=B*(DEF* SIN(RADS1-PHI)-EFG* COS(RADS1-PHI))
      AMP3=CONC* EXP(POW*TIME1)+BIT-2.0*DCVO/(3.0*OHM)
      COND=AMP3+B*HAB* COS(PHI)-B*GHI* SIN(PHI)+DCVO/(2.0*OHM)
```

```
      PLUS=-B*GHI* SIN(ANGLE-PHI)-B*HAB* COS(ANGLE-PHI)
      AMP4=COND* EXP(POW*PERIO)+PLUS-(DCVO/(2.0*OHM))
      PQR= SIN(ALPHA)
      QRS= COS(ALPHA)
      TILE=B*(PQR* SIN(PHI)+QRS* COS(PHI))
      PON=AMP4+TILE+DCVO/(3.0*OHM)
      ADD=B*(PQR* SIN(RADS1-PHI)-QRS* COS(RADS1-PHI))
      AMP5=PON* EXP(POW*TIME1)+ADD-DCVO/(3.0*OHM)
      FIX=PON* EXP(POW*TIME1)
      IF(W-1.0)304,948,948
  948 WRITE(6,100)AMP1,AMP2,AMP3,AMP4,AMP5,GAMA,CONA,CONB,CONC,COND,PON
  100 FORMAT(1H ,F8.3,2X,3F10.3,1X,F10.3,4X,F6.2,5F10.5)
  958 FORMAT(5F10.5)
      WRITE(6,958)PORT1,PICE2,BIT,PLUS,ADD
  304 IF(AMP5+0.01)7,8,8
    7 GAMA=GAMA+1.0
      IF(N-50)9,994,994
    9 N=N+1
      GOTO10
    8 WRITE(6,40)
   40 FORMAT(1H1,14H VALUE OF GAMA)
   41 WRITE(6,15)GAMA
   15 FORMAT(F10.2)
      GO TO 970
  994 WRITE(6,119)
  119 FORMAT(1H0,20HINVERSION IMPOSSIBLE)
      GO TO 75
  970 IF(W-1.0)12,940,940
  940 WRITE(6,16)
   16 FORMAT(1H1,50H CURRENT CONDUCTION PATTERN IN ELEMENT 2 OF BRIDGE)
      WRITE(6,951)
  951 FORMAT(1H0,20X,52H DEGREES FROM FIRING   ORDINATE  TRANSIENT  AC C
     1OMPO)
   12 IF(DELAY-210.0)920,920,921
  920 THETA=0.0
      ZEX=-(210.0-DELAY)*3.1428/180.0
      GO TO 96
  921 THETA=(DELAY-240.0+30.0)
      ZEX=0.0
   96 RISE=1.0
      FACT=1.0
      M=1
      J=11
      DIMENSIONC(12),SUM(12)
  900 DO 24 L=M,J,2
      ORD=0.0
   28 RADI=(RISE/180.0)*3.1428
      DEGRE=((RISE+THETA)*0.01746031)*FACT
      TAP=RADI/OMEGA
      IF(RISE-GAMA)29,30,30
   29 U=CONA* EXP(POW*TAP)
      V=B*(ABC* SIN(RADI-PHI)-BCD* COS(RADI-PHI))
      Y=U+V-DCVO/(3.0*OHM)
      IF(1-M)401,901,901
  901 IF(FACT-1.0)107,107,108
  107 IF(W-1.0)108,600,600
  600 WRITE(6,400)RISE,Y,U,V
  108 PROD=SIN(DEGRE)*Y
```

```
      GO TO750
  401 PROD=COS(DEGRE)*Y
  750 ORD=ORD+PROD
      RISE=RISE+1.0
      GOTO28
   30 RADI=(RISE-GAMA)*3.1428/180.0
      DEGRE=((RISE+THETA)*0.01746031)*FACT
      TAP=RADI/OMEGA
      U=CONB* EXP(POW*TAP)
      V=B*(CDE* SIN(RADI-PHI)+XYZ* COS(RADI-PHI))
      Y=U-V-DCVO/(2.0*OHM)
      IF(1-M)402,902,902
  902 IF(FACT-1.0)109,109,110
  109 IF(W-1.0)110,601,601
  601 WRITE(6,400)RISE,Y,U,V
  110 PROD=SIN(DEGRE)*Y
      GO TO 751
  402 PROD=COS(DEGRE)*Y
  751 ORD=ORD+PROD
      RISE=RISE+1.0
      IF(RISE-60.0)13,14,14
   13 GOTO30
   14 RADI=(RISE-60.0)*3.1428/180.0
      DEGRE=((RISE+THETA)*0.01746031)*FACT
      TAP=RADI/OMEGA
      U=CONC* EXP(POW*TAP)
      V=B*(DEF* SIN(RADI-PHI)-EFG* COS(RADI-PHI))
      Y=U+V-(2.0*DCVO)/(3.0*OHM)
      IF(1-M)403,903,903
  903 IF(FACT-1.0)111,111,112
  111 IF(W-1.0)112,602,602
  602 WRITE(6,400)RISE,Y,U,V
  112 PROD=SIN(DEGRE)*Y
      GO TO 752
  403 PROD=COS(DEGRE)*Y
  752 ORD=ORD+PROD
      RISE=RISE+1.0
      IF(RISE-60.0-GAMA)17,21,21
   17 GOTO14
   21 RADI=(RISE-60.0-GAMA)*3.1428/180.0
      DEGRE=((RISE+THETA)*0.01746031)*FACT
      TAP=RADI/OMEGA
      U=COND* EXP(POW*TAP)
      V=B*(GHI* SIN(RADI-PHI)+HAB* COS(RADI-PHI))
      Y=U-V-DCVO/(2.0*OHM)
      IF(1-M)405,904,904
  904 IF(FACT-1.0)113,113,114
  113 IF(W-1.0)114,603,603
  603 WRITE(6,400)RISE,Y,U,V
  114 PROD=SIN(DEGRE)*Y
      GO TO 753
  405 PROD=COS(DEGRE)*Y
  753 ORD=ORD+PROD
      RISE=RISE+1.0
      IF(RISE-120.0)19,18,18
   19 GO TO 21
   18 RISE=120.0
  103 RADI=(RISE-120.0)*3.1428/180.0
```

```
      DEGRE=((RISE+THETA)*0.01746031)*FACT
      TAP=RADI/OMEGA
      U=PON* EXP(POW*TAP)
      V=B*(PQR* SIN(RADI-PHI)-QRS* COS(RADI-PHI))
      Y=U+V-DCVO/(3.0*OHM)
      IF(1-M)404,905,905
  905 IF(FACT-1.0)115,115,116
  115 IF(W-1.0)116,604,604
  604 WRITE(6,400)RISE,Y,U,V
  116 PROD=SIN(DEGRE)*Y
      GO TO 754
  404 PROD=COS(DEGRE)*Y
  754 ORD=ORD+PROD
      RISE=RISE+1.0
      IF(RISE-121.0-GAMA)22,23,23
   22 GOTO103
   23 SUM(L)=ORD
      RISE=1.0
   24 FACT=FACT+2.0
      M=M+1
      J=12
      IF(M-2)700,700,702
  700 FACT=1.0
      GO TO 900
  702 DO27J=1,12,1
   27 C(J)=SUM(J)/90.0
      WRITE(6,62)S
   62 FORMAT(1H1,66H FOURIER COEFFICIENTS OF CURRENT IN ELT.2 OF BRIDGE
     1AT MOTOR SLIP=,F7.4)
      WRITE(6,502)
  502 FORMAT(1HO,43X,52H   FUNDL   THIRD  FIFTH    SEVENTH  NINETH  ELEV
     1ENTH)
      WRITE(6,953)
  953 FORMAT(1H ,18H SINE COEFFICIENTS)
      WRITE(6,63)C(1),C(3),C(5),C(7),C(9),C(11)
   63 FORMAT(1HO,43X,F8.3,F8.3,2X,F8.3,F9.3,F8.2,F10.3)
      WRITE(6,954)
  954 FORMAT(1H ,20H COSINE COEFFICIENTS)
      WRITE(6,63)C(2),C(4),C(6),C(8),C(10),C(12)
      WRITE(6,955)
  955 FORMAT(1HO,28H FOR INVERTER PARAMETERS OF-)
      WRITE(6,509)
  509 FORMAT(98H  DCVOLTS     ACVOLT      BETA        GAMA  XS REF ROTOR
     1   XR REF ROTOR  RS RE ROTOR   RR RE ROTOR)
      WRITE(6,501)DCVO,ACVO,DELAY,GAMA,HEN1,HEN2,OHM1,OHM2
  501 FORMAT(1H ,F8.3,3X,F8.2,4X,F7.1,4X,F8.2,F10.5,3X,F10.5,3X,F9.5,3X,
     1F9.5)
  400 FORMAT(1H ,20X,F8.3,12X,F10.5,1X,F10.5,2X,F8.3)
      IF(210.0-DELAY)31,31,32
   31 WRITE(6,90)
   90 FORMAT(53HOREFERENCE FOR COEFFICIENTS,240 DEGREE FROM REFERENCE)
      WRITE(6,91)
   91 FORMAT(33H AXIS THAT IS,FROM T=0 OF PHASE B)
      THETA=(DELAY-240.0+30.0)*3.1228/180.0
      GO TO175
   32 WRITE(6,92)
   92 FORMAT(1HO,47H REFERENCE FOR COEFFICIENTS IS DELAY+30 DEGREES)
      WRITE(6,93)
```

```
93 FORMAT(46H                                  FROM  T=0 OF RED PHASE)
```

The control number W can be either 0.0 or 1.0. If W is 1.0, the on line printer on the computer prints out the interval currents at each value of assumed γ and if the current at the end of interval 5 converges to zero, the ordinates for plotting the conduction pattern are printed. In addition, the value of γ, the Fourier coefficients of the current conduction pattern and the parameters of inversion are printed. If W = 0.0, only the value of γ, the Fourier coefficients of the current pattern and the parameters of inversion are printed.

The value of γ is incremented in steps of one degree and since γ cannot exceed 60 degrees, after 59 increments, if the current at the end of interval 5 does not converge to zero, a message "Inversion impossible" is printed on the printer.

7.4 Transformation of Phase Currents to d and q Axes of an Induction Motor

7.4.1 d and q transformations of the induction motor[11]

The d and q axes are chosen 90 degrees apart in space and rotating at synchronous speed corresponding to the electrical angular velocity ω of the impressed stator voltages.

When the d axis is so placed that it coincides with the axis of phase A at t=0, its displacement from the phase A at any time t is ωt. The corresponding displacements from the phase B and C axes are $(\omega t - 120^{o})$ and $(\omega t + 120^{o})$. The respective q axis displacements are 90 degrees greater than

those of the d axis. With all the 3 stator phases excited, the component mmfs along the d and q axes are then

$$F_{ds} = N\left[i_A \cos \omega t + i_B \cos(\omega t - 120^\circ) + i_C \cos(\omega t + 120^\circ)\right] \quad (7.43)$$

$$F_{qs} = N\left[-i_A \sin \omega t - i_B \sin(\omega t - 120^\circ) - i_C \sin(\omega t + 120^\circ)\right] \quad (7.44)$$

where N represents the effective turns per phase.

The stator current variables i_{ds} and i_{qs} may now be defined in terms of the bracketed quantities in equations (7.43) and (7.44), with an arbitrary constant multiplier K. Thus,

$$\begin{bmatrix} i_{ds} \\ -i_{qs} \end{bmatrix} = K \begin{bmatrix} \cos \omega t & \cos(\omega t - 120^\circ) & \cos(\omega t + 120^\circ) \\ \sin \omega t & \sin(\omega t - 120^\circ) & \sin(\omega t + 120^\circ) \end{bmatrix} \times \begin{bmatrix} i_A \\ i_B \\ i_C \end{bmatrix} \quad (7.45)$$

Exactly the same transformations can be made for the stator phase voltages V_A, V_B and V_C in terms of V_{ds} and V_{qs}.

Similarly, the rotor mmfs are resolved along two mutually perpendicular stator d and q axes. Let θ_s be the angle from the phase A axis of the rotor to the d axis. If the rotor is revolving at slip s, the d axis is advancing continuously with respect to a point in the rotor at the rate

$$\frac{d\theta_s}{dt} = p\theta_s = s\omega \quad (7.46)$$

Accordingly, the subscript s on the angle θ_s stands for slip. The rotor mmf components can then be expressed by equation (7.45) but with θ_s in place of ωt.

7.4.2 Evaluation of the constant K

The three phase induction motor can now be represented by an equivalent machine with two rotor and stator coils along the d and q axes revolving at the synchronous angular velocity of a two pole machine. If the operation of the motor is to be exactly described by the equivalent machine, the power input to the three phase machine should be equal to the power input to the equivalent machine. The equivalent machine has two poles and the d and q axes are rotating at the synchronous speed of a two pole machine. Let the maximum values of the phase voltages and currents of the three phase machine be V_m and i_m. Under balanced conditions, the values of i_{ds} and V_{ds} from equation (7.43) will be zero, and the values of V_{qs} and i_{qs} will be $3KV_m/2$ and $3Ki_m/2$ (eqn. (7.44)) respectively. The power input to the three phase machine per pole is $3V_A i_A/P$ where P is the number of pairs of poles. The power input to the equivalent machine per pole is the sum of $V_{ds}i_{ds}$ and $V_{qs}i_{qs}$. Hence, for invariance of power

$$\frac{3V_A i_A}{P} = \frac{3KV_m}{2}\ \frac{3Ki_m}{2} \qquad (7.47)$$

Since V_A and i_A are the RMS values of phase voltages and currents, equation (7.47) may be written as

$$\frac{3V_m i_m}{2P} = \frac{9K^2 V_m i_m}{4} \qquad (7.48)$$

or

$$K^2 = \frac{2}{3P} \qquad (7.49)$$

Therefore,

$$K = \sqrt{\frac{2}{3P}} \qquad (7.50)$$

For the laboratory machine used for the experimental verifications, P = 3 and, therefore,

$$K = 0.4714$$

7.5 Solution of Torque Equations

It has been shown in Section 3.3 that

$$i_{qs} = \frac{M(-\omega^2 L_1 - R_1 p - p^2 L_1) i_{qr} - \omega M R_1 i_{dr} + V_{qs} R_1}{(R_1 + pL_1)^2 + \omega^2 L_1^2} \qquad (3.19)$$

and

$$i_{ds} = \frac{M(-pR_1 + p^2 L_1 - \omega^2 L_1) i_{dr} + \omega M R_1 i_{qr} + V_{qs} \omega L_1}{(R_1 + pL_1)^2 + \omega^2 L_1^2} \qquad (3.26)$$

In Section 3.3, i_{dr} and i_{qr} have been shown to be

$$i_{dr} = K\left[1.5 I_1 \mathrm{Sin}(-\phi_1) + I_{6Rd} \mathrm{Sin}(6s\omega t - \phi_{Rd})\right] \qquad (3.17)$$

and

$$-i_{qr} = K\left[1.5 I_1 \mathrm{Cos}(-\phi_1) + I_{6Rq} \mathrm{Cos}(6s\omega t - \phi_{Rq})\right] \qquad (3.18)$$

The expressions for i_{dr} and i_{qr} each contain a d.c. component and an a.c. component of an angular velocity $6s\omega$. In the solution of (3.19) the d.c. terms come only from the d.c. quantities in equations (3.17) and (3.18) and from the term

$V_{qs}R_1$ in equation (3.19). The terms with coefficients p (where $p = \frac{d}{dt}$) do not contribute to any d.c. terms since the derivative of a d.c. term is zero. Solution of (3.19) for the d.c. term results in:

$$i_{\alpha 1} = \frac{-\omega^2 ML_1 i_{qr} - \omega MR_1 i_{dr} + V_{qs}R_1}{(R_1 + pL_1)^2 + \omega^2 L_1^2} \qquad (7.51)$$

Substituting the d.c. values for i_{qr} and i_{dr} from equations (3.17) and (3.18) and solving for each term in the numerator of equation (7.51) by the method of Laplace transforms, one gets

$$i_{\alpha 1} = i_{\alpha 10} + i_{\alpha 11} + i_{\alpha 12} \qquad (7.52)$$

where,

$$i_{\alpha 10} = \frac{+\omega^2 ML_1 1.5KI_1 \cos(-\phi_1)}{(R_1+pL_1)^2 + \omega^2 L_1^2} = \frac{+\omega^2 ML_1 1.5KI_1 \cos\phi_1}{R_1^2 + \omega^2 L_1^2} \qquad (7.53)$$

$$i_{\alpha 11} = \frac{- MR_1 K1.5I_1 \sin(-\phi_1)}{(R_1+pL_1)^2 + \omega^2 L_1^2} = \frac{- MR_1 K1.5I_1 \sin(-\phi_1)}{R_1^2 + \omega^2 L_1^2} \qquad (7.54)$$

and

$$i_{\alpha 12} = \frac{V_{qs}R_1}{(R_1 + pL_1)^2 + \omega^2 L_1^2} = \frac{V_{qs}R_1}{(R_1^2 + \omega^2 L_1^2)} \qquad (7.55)$$

Combining 7.53, 7.54 and 7.55, the d.c. component $i_{\alpha 1}$ is,

$$i_{\alpha 1} = \frac{V_{qs}R_1 + 1.5KI_1M(\omega^2 L_1 \cos\phi_1 - \omega R_1 \sin(-\phi_1))}{R_1^2 + \omega^2 L_1^2} \qquad (7.56)$$

The solution of (3.19) for the a.c. quantities will contain the a.c. component contributions from equations (3.17) and (3.18). Solution of (3.19) for i_{qs} results in

$$i_{qs} = \frac{M(-\omega^2 L_1 - R_1 p - p^2 L_1) i_{qr} - \omega M R_1 i_{dr}}{(R_1 + pL_1)^2 + \omega^2 L_1} \qquad (7.57)$$

Substituting the a.c. values for i_{qr} and i_{dr} from equations (3.17) and (3.18) and solving (7.57) for each term on the numerator, one gets

$$\frac{\omega^2 M L_1 K I_{6Rq} \cos(6s\omega t - \phi_{Rq})}{(R_1 + pL_1)^2 + \omega^2 L_1} = \frac{\omega^2 M L_1 I_{6Rq} K \cos(6s\omega t - \phi_{Rq} - \delta)}{Q} \qquad (7.58)$$

where,

$$\delta = \tan^{-1} \frac{2L_1 R_1 s}{(R_1^2 + {}^2L_1^2 - 36s^2\omega^2 L_1^2)} \qquad (7.59)$$

and

$$Q = \sqrt{(R_1^2 + \omega^2 L_1^2 - 36s^2\omega^2 L_1^2)^2 + 36 L_1^2 R_1^2 s^2 \omega^2} \qquad (7.60)$$

$$\frac{M R_1 p K I_{6Rq} \cos(6s\omega t - \phi_{Rq})}{(R_1 + pL_1)^2 + \omega^2 L_1} = \frac{-R_1 K I_{6Rq} M 6s\omega \sin(6s\omega t - \phi_{Rq} - \delta)}{Q} \qquad (7.61)$$

$$\frac{p^2 L_1 M K I_{6Rq} \cos(6s\omega t - \phi_{Rq})}{(R_1 + pL_1)^2 + \omega^2 L_1} = \frac{-K L_1 M I_{6Rq} 36 s^2 \omega^2 \cos(6s\omega t - \phi_{Rq} - \delta)}{Q} \qquad (7.62)$$

and

$$\frac{-\omega MR_1 KI_{6Rd}\mathrm{Sin}(6s\omega t-\phi_{Rd}-\delta)}{(R_1 + pL_1)^2 + \omega^2 L_1} = \frac{-\omega MKR_1 I_{6Rd}\mathrm{Sin}(6s\omega t-\phi_{Rd}-\delta)}{Q} \quad (7.63)$$

Combining (7.58), (7.61), (7.62) and (7.63) to evaluate the net a.c. term, one gets

$$i_{\beta 1} = \frac{-K}{Q}\Big\{I_{6Rq}M\Big[R_1 6s\omega\mathrm{Sin}(6s\omega t-\phi_{Rq}-\delta) - \omega^2 L_1\mathrm{Cos}(6s\omega t-\phi_{Rq}-\delta) + L_1 36s^2\omega^2\mathrm{Cos}(6s\omega t-\phi_{Rq}-\delta)\Big] + I_{6Rd}\omega MR_1\mathrm{Sin}(6s\omega t-\phi_{Rd}-\delta)\Big\} \quad (7.64)$$

The complete solution for i_{qs} is

$$i_{qs} = i_{\alpha 1} + i_{\beta 1} \quad (7.65)$$

Similarly, the solution for i_{ds} from equation (3.26) can be shown to be

$$i_{ds} = i_{\alpha 2} + i_{\beta 2} \quad (7.66)$$

where,

$$i_{\alpha 2} = \frac{V_{qs}\omega L_1 - 1.5KI_1 M(\omega R_1\mathrm{Cos}\phi_1 + \omega^2 L_1\mathrm{Sin}(-\phi_1))}{(R_1^2 + \omega^2 L_1^2)} \quad (7.67)$$

and

$$i_{\beta 2} = \frac{-K}{Q}\Big\{I_{6Rd}M\Big[R_1 6s\omega\mathrm{Cos}(6s\omega t-\phi_{Rd}-\delta) + L_1 36s^2\omega^2\mathrm{Sin}(6s\omega t-\phi_{Rd}-\delta) + \omega^2 L_1\mathrm{Sin}(6s\omega t-\phi_{Rd}-\delta)\Big] + I_{6Rq}\omega MR_1\mathrm{Cos}(6s\omega t-\phi_{Rq}-\delta)\Big\} \quad (7.68)$$

7.6 Digital Computer Program for the Solution of Stator d and q Currents

The equations derived for i_{qs} and i_{ds} in Section 7.5 are evaluated using a digital computer. The program, essentially, evaluates the various d.c. and a.c. components given by equations (7.53), (7.54), (7.55), (7.58), (7.61), (7.62) and (7.63). The components are summed to get the net d.c. and a.c. currents according to equations (7.56), (7.67) and (7.64), (7.68) respectively.

Fig. 7.5 indicates in a block diagram the logic of the program and the statements in Fortran IV language are also listed. The program is written as a continuation to the program for the solution of the conduction equations (Section 7.3). The program, in addition to the evaluation of the stator currents, is written to calculate the torque of the induction motor on the basis of equation (3.35). A sample print out on the on line printer of the IBM 7040 computer is also shown in Table 7.3.

7.7 Transformation of Rotor Harmonic Currents to Two Synchronously Rotating Axes

The synchronously revolving axes along which the phase currents are transformed are designated as d and q axes.

Let the three rotor phase currents be

$$I_{rA} = I_n \text{ Sin } (n\omega_r t - \phi_n) \tag{7.69}$$

$$I_{rB} = I_n \text{ Sin } (n\omega_r t - 120^\circ n - \phi_n) \tag{7.70}$$

$$I_{rC} = I_n \text{ Sin } (n\omega_r t + 120^\circ n + \phi_n) \tag{7.71}$$

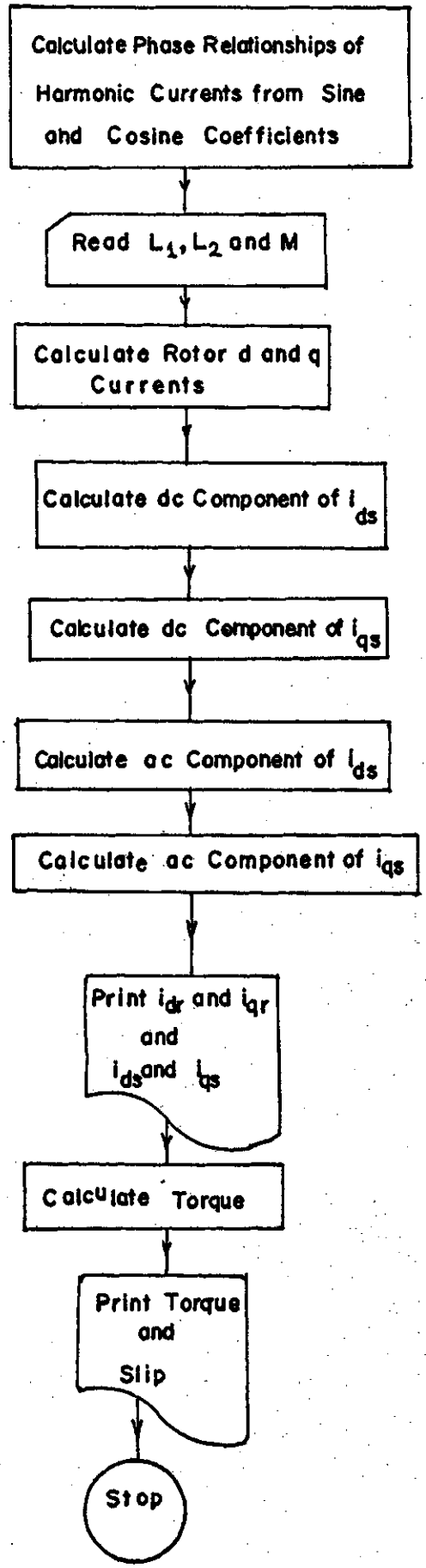

Figure 7·5 Block Diagram of Logic for the Solution of Torque Equations

Table 7.2, Card Listings of the Program for the Solution of Torque Equations

```
175 PATRIX=1.5*0.4714
    V1Q=(PATRIX*SQRT(2.0)*ACVO)
    VECT1=CMPLX(C(1),C(2))
    VECT3=CMPLX(C(3),C(4))
    VECT5=CMPLX(C(5),C(6))
    VECT7=CMPLX(C(7),C(8))
    VECT9=CMPLX(C(9),C(10))
    VECT11=CMPLX(C(11),C(12))
    A1=CABS(VECT1)
    A3=CABS(VECT3)
    A5=CABS(VECT5)
    A7=CABS(VECT7)
    A9=CABS(VECT9)
    A11=CABS(VECT11)
    EFFECT=SQRT(A1**2.0+A3**2.0+A5**2.0+A7**2.0+A9**2.0+A11**2.0)
    WRITE(6,993)EFFECT
993 FORMAT(37H EFFECTIVE VALUE OF ROTOR CURRENTS IS,F10.3,7H AMPRES)
    READ(5,300)DUTH,OHMEQ1,HENQT1
300 FORMAT(3F9.5)
    DUTUAL=DUTH/OMEGAS
    HENEQ1=HENQT1/OMEGAS
    OUT=6.0*S*OMEGAS
    DCD=A1*PATRIX
    AC5=A5*PATRIX
    AC7=A7*PATRIX
    A1=CABS(VECT1)*PATRIX
    A6=CABS(VECT5)*PATRIX
    A7=CABS(VECT7)*PATRIX
    PHI1=ATAN2(C(2),C(1))+ZEX
    PHI5=ATAN2(C(6),C(5))+ZEX
    PHI7=ATAN2(C(8),C(7))+ZEX
    AIDC=DCD*SIN(PHI1)
    BIDC=DCD*COS(PHI1)*(-1.0)
    TRUE6=AC5*COS(PHI5)
    HA6=AC5*SIN(PHI5)
    TRUE7=AC7*COS(PHI7)
    HA7=AC7*SIN(PHI7)
    CMVEA=CMPLX(TRUE6,HA6)
    CMVEB=CMPLX(TRUE7,HA7)
    AB=CMVEA+CMVEB
    BB=CMVEB-CMVEA
    PHI6A=ATAN2(AIMAG(AB),REAL(AB))
    PHI6B=ATAN2(AIMAG(BB),REAL(BB))
    A2=CABS(AB)
    B2=CABS(BB)*(-1.0)
    WRITE(6,299)
    WRITE(6,299)
    WRITE(6,120)
    WRITE(6,121)AIDC,A2,OUT,PHI6A
    WRITE(6,122)BIDC,B2,OUT,PHI6B
    DENOM=OHMEQ1**2.0+(OMEGAS*HENEQ1)**2.0
    DCCM11=BIDC*DUTUAL*OMEGAS*OHMEQ1/DENOM
    DCCM12=DUTUAL*HENEQ1*AIDC*(OMEGAS**2.0)/DENOM
    DCCM13=V1Q*OMEGAS*HENEQ1/DENOM
    DCCMRE=DCCM11-DCCM12+DCCM13
    HUMRT=2.0*6.0*OMEGAS*OHMEQ1*HENEQ1*S
```

```
DOWN=(OMEGAS**2.0)*HENEQ1**2.0*(1.0-36.0*S**2.0)+OHMEQ1**2.0
RHO=ATAN2(HUMRT,DOWN)
SHIBE=OMEGAS**2.0*(HENEQ1**2.0)*(S**2.0)*36.0
DIVID=DENOM-SHIBE
RDID=(OHMEQ1**2.0)*SHIBE*4.0
STELLE=ABS(DIVID)
ZN=DUTUAL/SQRT(STELLE**2.0+RDID)
TRUNK=OMEGAS**2.0*(A2*HENEQ1)*ZN
BRINK=A2*OHMEQ1*6.0*S*OMEGAS*ZN
DELTA=PHI6A-RHO
STAR=COS(DELTA)
STAJ=SIN(DELTA)
STBR=36.0*S**2.0*(COS(DELTA))
STBJ=36.0*S**2.0*(SIN(DELTA))
STCR=COS(DELTA+1.5714)
STCJ=SIN(DELTA+1.5714)
STDA=CMPLX(STAR,STAJ)
STDB=CMPLX(STBR,STBJ)
STDC=CMPLX(STCR,STCJ)
STM1=TRUNK*(STDA+STDB)
STM2=BRINK*STDC
STDR1=STM1+STM2
SIGMA=PHI6B-RHO
STER=COS(SIGMA)
STEJ=SIN(SIGMA)
STDD=CMPLX(STER,STEJ)
STDR2=(OMEGAS*OHMEQ1*B2*ZN)*STDD
STDRES=STDR2-STDR1
ACRES=CABS(STDRES)
ACPHID=ATAN2(AIMAG(STDRES),REAL(STDRES))
WRITE(6,125)
WRITE(6,121)DCCMRE,ACRES,OUT,ACPHID
DCCM21=(OMEGAS**2.0)*HENEQ1*DUTUAL*BIDC/DENOM
DCCM22=OMEGAS*OHMEQ1*DUTUAL*AIDC/DENOM
DCCM23=V1Q*OHMEQ1/DENOM
DCREQS=-DCCM21-DCCM22+DCCM23
FACTOR=B2*ZN
QUOTIE=A2*OMEGAS*ZN
SI=DELTA
TI=SIGMA
OAR=HENEQ1*OMEGAS**2.0*COS(TI)*FACTOR
OAJ=HENEQ1*OMEGAS**2.0*SIN(TI)*FACTOR
OBR=OHMEQ1*COS(TI-1.5714)*6.0*S*OMEGAS*FACTOR
OBJ=OHMEQ1*SIN(TI-1.5714)*6.0*S*OMEGAS*FACTOR
OCJ=HENEQ1*SIN(TI)        *36.0*S**2.0*(OMEGAS**2.0)*FACTOR
OCR=HENEQ1*COS(TI)        *36.0*S**2.0*(OMEGAS**2.0)*FACTOR
ACA=CMPLX(OAR,OAJ)
ACB=CMPLX(OBR,OBJ)
ACC=CMPLX(OCR,OCJ)
ACQR1=(ACB+ACC-ACA)
ODR=OHMEQ1*COS(SI)
ODJ=OHMEQ1*SIN(SI)
OER=QUOTIE*ODR
OEJ=QUOTIE*ODJ
ACE=CMPLX(OER,OEJ)
ACNETC=ACQR1-ACE
ACNETQ=CABS(ACNETC)
ACPHIQ=ATAN2(AIMAG(ACNETC),REAL(ACNETC))
```

```
      WRITE(6,122)DCREQS,ACNETQ,DUT,ACPHIQ
      OPTAF=AIDC*DCREQS
      OPTBF=BIDC*DCCMRE
      OPTAH=A2*ACNETQ*SIN(PHI6A-ACPHIQ)/2.0
      OPTBH=B2*ACRES*SIN(PHI6B-ACPHID)/2.0
      TQ=DUTUAL*3.0*(OPTBF-OPTAF)*OMEGAS*(00.00586)*S
      TQH=(OPTBH-OPTAH)*DUTUAL*OMEGAS*3.0*(00.00586)*S
      WRITE(6,708)TQ,TQH
  708 FORMAT(1HO,13HFUNDL TORQUE=,F10.2,27HFOOT LBS.  HARMONIC TORQUE=,F
     110.5,9HFOOT LBS.)
 1200FORMAT(1HO,112H ROTOR CURRENTS OF INDUCTION MOTOR WITH INVERTER IN
     I THE ROTOR REFERED TO TWO SYNCHRONOUSLY ROTATING D AND Q AXES)
 1210FORMAT(1HO,20HDIRECT AXIS CURRENT=,F10.2,2H +,F10.2,4HSIN(,F10.2,2
     1HT+,F10.2,1H))
 1220FORMAT(1H ,19HQUADR AXIS CURRENT=,F10.2,2H +,F10.2,4HSIN(,F10.2,2H
     1T+,F10.2,1H))
  125 FORMAT(1HO,58H STATOR CURRENTS REFERED TO THE SAME PAIR OF ROTATIN
     1G AXES)
  299 FORMAT(1HO,3H    )
   75 STOP
      END
```

FOURIER COEFFICIENTS OF CURRENT IN ELT.2 OF BRIDGE AT MOTOR SLIP= 1.0000

	FUNDL	THIRD	FIFTH	SEVENTH	NINETH	ELEVENTH
SINE COEFFICIENTS	-19.504	-1.313	-2.564	-1.487	0.27	-0.188
COSINE COEFFICIENTS	-9.759	0.763	3.671	1.420	0.24	0.670

FOR INVERTER PARAMETERS OF-

DCVOLTS	ACVOLT	BETA	GAMA	XS REF ROTOR	XR REF ROTOR	RS RE ROTOR	RR RE ROTOR
132.500	138.01	210.0	23.20	0.00066	0.00084	0.14030	0.36300

REFERENCE FOR COEFFICIENTS,240 DEGREE FROM REFERENCE
AXIS THAT IS,FROM T=0 OF PHASE B
EFFECTIVE VALUE OF ROTOR CURRENTS IS 22.424 AMPRES

ROTOR CURRENTS OF INDUCTION MOTOR WITH INVERTER IN THE ROTOR REFERED TO TWO SYNCHRONOUSLY ROTATING D AND Q AXES

DIRECT AXIS CURRENT= -6.90 + 4.60SIN(2262.84T+ 2.24)
QUADR AXIS CURRENT= 13.79 + -1.76SIN(2262.84T+ -1.12)

STATOR CURRENTS REFERED TO THE SAME PAIR OF ROTATING AXES

DIRECT AXIS CURRENT= 13.49 + 4.64SIN(2262.84T+ 2.25)
QUADR AXIS CURRENT= -12.86 + 1.68SIN(2262.84T+ -1.12)

FUNDL TORQUE= 34.07FOOT LBS. HARMONIC TORQUE= -0.03834FOOT LBS.

TABLE 7.3: Output from the Computer

FOURIER COEFFICIENTS OF CURRENT IN ELT.2 OF BRIDGE AT MOTOR SLIP= 0.5000

	FUNDL	THIRD	FIFTH	SEVENTH	NINETH	ELEVENTH
SINE COEFFICIENTS	-10.866	-0.055	-5.315	0.250	-0.02	-1.005
COSINE COEFFICIENTS	-6.868	-0.027	1.256	1.739	0.02	0.779

FOR INVERTER PARAMETERS OF-

DCVOLTS	ACVOLT	BETA	GAMA	XS REF ROTOR	XR REF ROTOR	RS RE ROTOR	RR RE ROTOR
63.500	138.01	195.0	2.20	0.00066	0.00084	0.14000	0.56000

REFERENCE FOR COEFFICIENTS IS DELAY+30 DEGREES
FROM T=0 OF RED PHASE

EFFECTIVE VALUE OF ROTOR CURRENTS IS 14.134 AMPRES

ROTOR CURRENTS OF INDUCTION MOTOR WITH INVERTER IN THE ROTOR REFERED TO TWO SYNCHRONOUSLY ROTATING D AND Q AXES

DIRECT AXIS CURRENT= -2.70 + 4.16SIN(1131.42T+ 2.35)
QUADR AXIS CURRENT= 8.68 + -3.95SIN(1131.42T+ -0.18)

STATOR CURRENTS REFERED TO THE SAME PAIR OF ROTATING AXES

DIRECT AXIS CURRENT= 9.37 + 4.96SIN(1131.42T+ 2.37)
QUADR AXIS CURRENT= -8.07 + 3.76SIN(1131.42T+ -0.17)

FUNDL TORQUE= 10.43FOOT LBS. HARMONIC TORQUE= 0.15712FOOT LBS.

Contd:

TABLE 7.3: Output from the Computer

where I_n is the peak magnitude of the n^{th} harmonic current in the rotor, ϕ_n the phase relation of the n^{th} harmonic current with respect to the phase voltage, and ω_r the angular velocity corresponding to the frequency of rotor currents.

It has been shown in reference 11 that

$$\begin{vmatrix} i_{dr} \\ -i_{qr} \end{vmatrix} = K \begin{vmatrix} \cos\theta_s & \cos(\theta_s-120^\circ) & \cos(\theta_s+120^\circ) \\ \sin\theta_s & \sin(\theta_s-120^\circ) & \sin(\theta_s+120^\circ) \end{vmatrix} \times \begin{vmatrix} i_{rA} \\ i_{rB} \\ i_{rC} \end{vmatrix} \qquad (7.72)$$

where θ_s is the angle from the rotor phase A axis to the d axis. Under steady state conditions, if the rotor is revolving at a slip s, the d axis is advancing continuously with respect to a point on the rotor at a rate

$$\frac{d\theta_s}{dt} = p\theta_s = s\omega \qquad (7.73)$$

$s\omega$ being the frequency of rotor currents,

$$\theta_s = s\omega t = \omega_r t \qquad (7.74)$$

Therefore, transforming the phase currents given by (7.69), (7.70) and (7.71) to their d and q components using (7.72)

$$I_{dr} = KI_n\left[\sin(n\omega_r t-\phi_n)\cos\omega_r t + \sin(n\omega_r t-\tfrac{2\pi}{3}n-\phi_n)\cos(\omega_r t-\tfrac{2\pi}{3}) + \sin(n\omega_r t+\tfrac{2\pi}{3}n-\phi_n)\cos(\omega_r t+\tfrac{2\pi}{3})\right] \qquad (7.75)$$

A trigonometric simplification of (7.75) will yield,

$$i_{dr} = \sum_{1}^{n} K \frac{I_n}{2}\Big\{\Big(2\cos\Big[(n+1)\frac{2\pi}{3}\Big] + 1\Big)\Big(\sin\big[(n+1)\omega_r t - \phi_n\big]\Big)$$

$$+ \Big(2\cos\Big[(n-1)\frac{2\pi}{3}\Big] + 1\Big)\Big(\sin\big[(n-1)\omega_r t - \phi_n\big]\Big)\Big\} \qquad (7.76)$$

Similarly,

$$-i_{qr} = KI_n\Big[\sin(n\omega_r t-\phi_n)\sin\omega_r t + \sin(n\omega_r t-\frac{2\pi}{3}n-\phi_n)\sin(\omega_r t-\frac{2\pi}{3})$$

$$+ \sin(n\omega_r t+\frac{2\pi}{3}n-\phi_n)\sin(\omega_r t+\frac{2\pi}{3})\Big] \qquad (7.77)$$

Equation 7.77, upon simplification, reduces to

$$-i_{qr} = \sum_{1}^{n} K \frac{I_n}{2}\Big\{-\Big(2\cos\Big[\frac{2\pi}{3}(n+1)\Big] + 1\Big)\Big(\cos\big[(n+1)\omega_r t - \phi_n\big]\Big)$$

$$+ \Big(2\cos\Big[\frac{2\pi}{3}(n-1)\Big] + 1\Big)\Big(\cos\big[(n-1)\omega_r t - \phi_n\big]\Big)\Big\} \qquad (7.78)$$

Expressing (7.76) and (7.78) in matrix notation, the final equations will be,

$$\begin{vmatrix} i_{dr} \\ -i_{qr} \end{vmatrix} = \sum_{1}^{n} \frac{KI_n}{2} \begin{vmatrix} \sin\big[(n+1)s\omega t-\phi_n\big] & \sin\big[(n-1)s\omega t-\phi_n\big] \\ -\cos\big[(n+1)s\omega t-\phi_n\big] & \cos\big[(n-1)s\omega t-\phi_n\big] \end{vmatrix} \times \begin{vmatrix} 2\cos\big[(n+1)\frac{2\pi}{3}\big]+1 \\ 2\cos\big[(n-1)\frac{2\pi}{3}\big]+1 \end{vmatrix}$$

(7.79)